

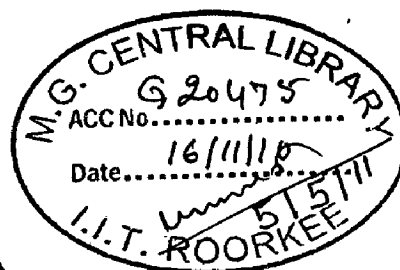
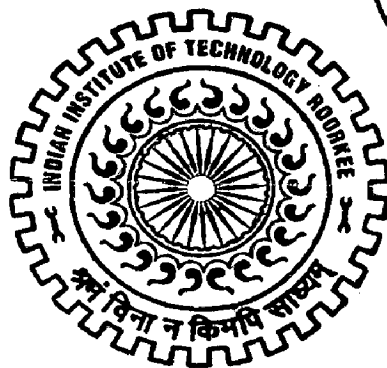
CONTROLLED RELEASE OF AMPHOTERICIN B FROM ELECTROSPUN NANOFIBER BASED ON GELATIN: A NEW INSIGHT TO DRUG DELIVERY AGAINST LESHMANIASIS

A DISSERTATION

*Submitted in partial fulfillment of the
requirements for the award of the degree
of
MASTER OF TECHNOLOGY
in
NANOTECHNOLOGY*

By

HIMANSU SEKHAR NANDA



CENTRE OF NANOTECHNOLOGY
INDIAN INSTITUTE OF TECHNOLOGY ROORKEE
ROORKEE-247 667 (INDIA)

JUNE, 2010

CANDIDATE'S DECLARATION

I hereby declare that the work presented in this dissertation report entitled, **“CONTROLLED RELEASE OF AMPHOTERICIN B FROM ELECTROSPUN NANOFIBER BASED ON GELATIN: A NEW INSIGHT TO DRUG DELIVERY AGAINST LESHMANIASIS”** towards the partial fulfillment of the requirements for the award of **Master of Technology in Nanotechnology**, submitted in the Center of Nanotechnology, Indian Institute of Technology Roorkee is an authentic record of my own work carried out during the period from July 2009 to June 2010, under the guidance of **Associate Professor R. Jayaganthan, Center of Nanotechnology and Assistant Professor Narayan Chandra Mishra, Department of Paper Technology, Indian Institute of Technology Roorkee, Uttarakhand, India.**

The content of this dissertation has not been previously submitted for examination as part of any academic qualifications.

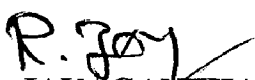
Date: 30th June 2010

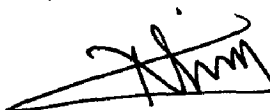
Place: Roorkee


HIMANSU SEKHAR NANDA

CERTIFICATE

This is to certify that the above statement made by the candidate is correct to the best of my knowledge and belief.


Dr. R. JAYAGANTHAN
Associate Professor,
Center of Nanotechnology,
Indian Institute of Technology, Roorkee


Dr. NARAYAN CHANDRA MISHRA
Assistant Professor,
Department of Paper Technology,
Indian Institute of Technology, Roorkee

ACKNOWLEDGEMENTS

This thesis concludes two years of study at the Indian Institute of Technology Roorkee. More importantly, it marks the end of another valuable chapter in my life. A journey is easier when you travel together. This thesis is the result of one year of work whereby I have been accompanied and supported by many people. It is a pleasant aspect that I have now the opportunity to express my gratitude to all of them.

I am greatly indebted to **Dr. R Jayaganthan** for being such a wonderful advisor. I thank him for his valuable guidance, support, discussions, encouragement and critical evaluation at each and every stage of my progress.

I am greatly indebted to my co- advisor **Dr. Narayan Chandra Mishra** for his valuable discussions, encouragement, his interest in my research work and providing me modern experimental facilities for carrying out such research.

I would like to express my sincere thanks to Dr. Anil Kumar, Head of Center of Nanotechnology for his valuable support and encouragement during the course of this dissertation.

I would like express my sincere thanks to Dean (SRIC), IIT Roorkee for providing the grant for electrospinning facility.

I would like to extend my thank to my lab research scholars for their constant support and Mr. Surendra Pratap Singh for valuable help during thesis preparation.

I feel a deep sense of gratitude for my mother, **Smt. Binodini Nanda** and father, **Mr. Pradipta Kumar Nanda** who formed part of my vision and taught me the lessons that really matter to my life. I am also grateful to my sisters Sasmita, Suchismita and my brother in law Govind for their constant support and valuable affection and inspiration.

Last but not the least; I thank **GOD** for giving me strength for overcoming the difficulties in my work front.

(HIMANSU SEKHAR NANDA)

CONTENTS	Page No.
ACKNOWLEDGEMENTS	iii
CONTENTS	iv
LIST OF FIGURES	vi
LIST OF TABLES	viii
LIST OF SYMBOLS/ABBREVIATIONS	ix
EXECUTIVE SUMMARY	x
CHAPTER 1: INTRODUCTION	1
CHAPTER 2: LITERATURE REVIEW	4
2.1 Introduction to leishmaniasis	4
2.1.1 Life cycle	5
2.1.1.1 Stages in invertebrate host.	5
2.1.1.2 Stages in vertebrate host	6
2.1.2 Clinical diversity in human	7
2.1.3 Taxonomy	7
2.1.4 Symptoms	8
2.1.5 Treatment	9
2.2 Electrospinning and nanofiber	9
2.2.1 Experimental set up	10
2.2.2 Physics of fiber formation	11
2.2.3 Process optimization	12
2.2.3.1 Processing Parameters	12
2.2.3.1.1 Applied voltage	12
2.2.3.1.2 Flow rate	12
2.2.3.1.3 Capillary to collector distance	13
2.2.3.2 Solution parameters	13
2.2.3.2.1 Polymer concentration	13
2.2.3.2.2 Solvent volatility	14
2.2.3.2.3 Solution conductivity	14
2.2.3.3 Ambient parameters	14
2.2.4 Characterization of nanofibers	14
2.2.5 Potential applications	15
2.2.5.1 Nanofiber reinforced composites	15
2.2.5.2 Nanofiber based membranes and smart cloths	16
2.2.5.3 Biomedical applications	16
2.2.5.3.1 Tissue engineering	16
2.2.5.3.2 Encapsulation of bioactive materials	17
2.2.5.3.3 Wound dressing	17
2.2.5.3.4 Medical prostheses	18
2.2.5.3.5 Cosmetics	18
2.2.5.4 Electrical and optical application	18
2.2.5.5 Filtration application	19
2.2.5.6 Other functional application	19
CHAPTER 3: EXPERIMENTAL	20
3.1 Materials	20

LIST OF FIGURES

Figure No.	Title	Page No.
2.1	Leishmania infantum (a) Amastigotes (b) Promastigotes	6
2.2	Life cycle of leishmaniasis	6
2.3	Taxonomy of <i>leishmania</i> spp.	8
2.4	Generic electro-spinning set-up depicting the major components of the electro-spinning process, including a high-voltage power supply, polymer solution and grounded collection target.	10
2.5	Photographs of typical electrospinning jets captured using a high-speed camera showing the electrically driven bending instability.	11
2.6	(a) SEM of PLLA nanofibers (b) TEM of elastin-mimetic peptide fibers (bar represents 3.3 nm) and (c) AFM of polyurethane nanofibers	15
3.1	Chemical Structure of (A) Gelatin and , (B) Amphotericin B	20
3.2	Electrospinning instrument of Tissue Engineering Laboratory, Department of Paper Technology, IIT Roorkee, Saharanpur Campus, which has been used for this work.	22
4.1	SEM images of amphotericin B loaded gelatin electrospun fibers from 8 wt% of gelatin in scale bar of 10 μm (A), 5 μm (B), 2 μm (C) and 1 μm (D).	26
4.2	SEM images of amphotericin B loaded gelatin electrospun fibers from 9 wt% of gelatin in scale bar of 10 μm (A), 5 μm (B), 2 μm (C) and 0.5 μm (D)	27
4.3	SEM images of amphotericin B loaded gelatin electrospun fibers from 10 wt% of gelatin in scale bar of 10 μm (A), 5 μm (B), 2 μm (C) and 0.5 μm (D)	28
4.4	SEM images of amphotericin B loaded gelatin electrospun fibers from 10 wt% of gelatin at flow rate 0.4 ml/hr in scale bar of 20 μm (A), 10 μm (B), 5 μm (C) and 2 μm (D)	30
4.5	SEM images of amphotericin B loaded gelatin electrospun fibers from 10 wt% of gelatin at flow rate 0.3ml/hr in scale bar of 20 μm (A), 10 μm (B), 5 μm (C) and 2 μm (D)	31
4.6	SEM images of amphotericin B loaded gelatin electrospun fibers from 10 wt% of gelatin at flow rate 0.2ml/hr in scale bar of 10 μm (A), 5 μm (B), 2 μm (C) and 1 μm (D)	32
4.7	SEM images of amphotericin B loaded gelatin electrospun fibers from 10 wt% of gelatin at flow rate 0.1ml/hr in scale bar of 10 μm (A) , 5 μm (B), 2 μm (C) and 1 μm (D)	33
4.8	SEM images of amphotericin B loaded gelatin electrospun fibers from 10 wt% of gelatin at flow rate: 0.1ml/hr, applied voltage: 20kV, TCD: 12cm in scale bar of 10 μm (A),5 μm (B),2 μm (C) and 1 μm (D)	35
4.9	SEM images of amphotericin B loaded gelatin electrospun fibers	36

CONTENTS

Page No.

ACKNOWLEDGEMENTS	iii
CONTENTS	iv
LIST OF FIGURES	vi
LIST OF TABLES	viii
LIST OF SYMBOLS/ABBREVIATIONS	ix
EXECUTIVE SUMMARY	x
CHAPTER 1: INTRODUCTION	1
CHAPTER 2: LITERATURE REVIEW	4
2.1 Introduction to leishmaniasis	4
2.1.1 Life cycle	5
2.1.1.1 Stages in invertebrate host.	5
2.1.1.2 Stages in vertebrate host	6
2.1.2 Clinical diversity in human	7
2.1.3 Taxonomy	7
2.1.4 Symptoms	8
2.1.5 Treatment	9
2.2 Electrospinning and nanofiber	9
2.2.1 Experimental set up	10
2.2.2 Physics of fiber formation	11
2.2.3 Process optimization	12
2.2.3.1 Processing Parameters	12
2.2.3.1.1 Applied voltage	12
2.2.3.1.2 Flow rate	12
2.2.3.1.3 Capillary to collector distance	13
2.2.3.2 Solution parameters	13
2.2.3.2.1 Polymer concentration	13
2.2.3.2.2 Solvent volatility	14
2.2.3.2.3 Solution conductivity	14
2.2.3.3 Ambient parameters	14
2.2.4 Characterization of nanofibers	14
2.2.5 Potential applications	15
2.2.5.1 Nanofiber reinforced composites	15
2.2.5.2 Nanofiber based membranes and smart cloths	16
2.2.5.3 Biomedical applications	16
2.2.5.3.1 Tissue engineering	16
2.2.5.3.2 Encapsulation of bioactive materials	17
2.2.5.3.3 Wound dressing	17
2.2.5.3.4 Medical prostheses	18
2.2.5.3.5 Cosmetics	18
2.2.5.4 Electrical and optical application	18
2.2.5.5 Filtration application	19
2.2.5.6 Other functional application	19
CHAPTER 3: EXPERIMENTAL	20
3.1 Materials	20

3.2 Characterization and spectroscopic techniques	21
3.3 Electrospinning	21
3.3.1 Preparation of drug loaded polymer solution	21
3.3.2 General procedure for electrospinning	22
3.3.3 Electrospinning Process optimization strategy	22
3.4 Chemical integrity of drug in drug loaded electrospun nanofiber	23
3.5 In-vitro drug release study	23
3.5.1 Preparation phosphate buffer solution	23
3.5.2 Preparation of standard calibration curve	23
3.5.3 Drug release assay	24
CHAPTER 4: RESULTS AND DISCUSSIONS	25
4.1 Electrospinning process optimization and morphology of drug loaded fiber mat	25
4.1.1 Effect of polymer concentration on fiber morphology	25
4.1.2 Effect of volume flow rate on fiber morphology	29
4.1.3 Effect of applied voltage and tip to collector distance on fiber morphology	34
4.2 Chemical integrity of drug in drug loaded gelatin nanofiber	38
4.3 In-vitro drug release study	40
4.3.1 Standard calibration curve preparation	40
4.3.2 Drug release assay	42
CHAPTER 5: SUMMARY	44
CHAPTER 6: CONCLUSION AND RECOMMENDATION	45
REFERENCES	46

LIST OF FIGURES

Figure No.	Title	Page No.
2.1	Leishmania infantum (a) Amastigotes (b) Promastigotes	6
2.2	Life cycle of leishmaniasis	6
2.3	Taxonomy of <i>leishmania</i> spp.	8
2.4	Generic electro-spinning set-up depicting the major components of the electro-spinning process, including a high-voltage power supply, polymer solution and grounded collection target.	10
2.5	Photographs of typical electrospinning jets captured using a high-speed camera showing the electrically driven bending instability.	11
2.6	(a) SEM of PLLA nanofibers (b) TEM of elastin-mimetic peptide fibers (bar represents 3.3 μm) and (c) AFM of polyurethane nanofibers	15
3.1	Chemical Structure of (A) Gelatin and , (B) Amphotericin B	20
3.2	Electrospinning instrument of Tissue Engineering Laboratory, Department of Paper Technology, IIT Roorkee, Saharanpur Campus, which has been used for this work.	22
4.1	SEM images of amphotericin B loaded gelatin electrospun fibers from 8 wt% of gelatin in scale bar of 10 μm (A), 5 μm (B), 2 μm (C) and 1 μm (D).	26
4.2	SEM images of amphotericin B loaded gelatin electrospun fibers from 9 wt% of gelatin in scale bar of 10 μm (A), 5 μm (B), 2 μm (C) and 0.5 μm (D)	27
4.3	SEM images of amphotericin B loaded gelatin electrospun fibers from 10 wt% of gelatin in scale bar of 10 μm (A), 5 μm (B), 2 μm (C) and 0.5 μm (D)	28
4.4	SEM images of amphotericin B loaded gelatin electrospun fibers from 10 wt% of gelatin at flow rate 0.4 ml/hr in scale bar of 20 μm (A), 10 μm (B), 5 μm (C) and 2 μm (D)	30
4.5	SEM images of amphotericin B loaded gelatin electrospun fibers from 10 wt% of gelatin at flow rate 0.3ml/hr in scale bar of 20 μm (A), 10 μm (B), 5 μm (C) and 2 μm (D)	31
4.6	SEM images of amphotericin B loaded gelatin electrospun fibers from 10 wt% of gelatin at flow rate 0.2ml/hr in scale bar of 10 μm (A), 5 μm (B), 2 μm (C) and 1 μm (D)	32
4.7	SEM images of amphotericin B loaded gelatin electrospun fibers from 10 wt% of gelatin at flow rate 0.1ml/hr in scale bar of 10 μm (A) , 5 μm (B), 2 μm (C) and 1 μm (D)	33
4.8	SEM images of amphotericin B loaded gelatin electrospun fibers from 10 wt% of gelatin at flow rate: 0.1ml/hr, applied voltage: 20kV, TCD: 12cm in scale bar of 10 μm (A),5 μm (B),2 μm (C) and 1 μm (D)	35
4.9	SEM images of amphotericin B loaded gelatin electrospun fibers	36

	from 10 wt% of gelatin at flow rate: 0.1ml/hr, applied voltage: 20kV, TCD: 13.5cm in scale bar of 5 μm (A), 2 μm (B), 2 μm (C) and, 1 μm (D)	
4.10	SEM images of amphotericin B loaded gelatin electrospun fibers from 10 wt% of gelatin at flow rate: 0.1ml/hr, applied voltage: 16kV, TCD: 13.5cm in scale bar of 10 μm (A), 5 μm (B), 2 μm (C) and, 1 μm (D)	37
4.11	FTIR spectra of pure amphotericin B	38
4.12	FTIR spectra of pure gelatin nanofiber mat.	39
4.13	FTIR Spectra of amphotericin B loaded gelatin nanofiber mat	39
4.14	Standard calibration curve for the known drug concentrations	41
4.15	Drug release profile of amphotericin B in 12 hours	42

LIST OF TABLES

Table No.	Title	Page No.
3.1	Different composition of gelatin, amphotericin B, acetic acid and water in the solution.	21
3.2	Composition of drug, PBS in the different concentration solution	24
4.1	UV-Vis spectra analysis at different concentration of drug.	40
4.2	Observation of drug release in different time by UV-Vis spectroscopy	42

LIST OF SYMBOLS/ABBREVIATIONS

ACK	Acknowledgement
KA	Kala-Azar
VL	visceral leshmaniasis
CL	cutaneous leshmaniasis
Sb (V)	pentavalent antimonials
SAG	Sodium Antimony Gluconate
DDs.	drug delivery system
FE-SEM	Field Emission Scanning Electron Microscopy
FTIR	Fourier Transformation Infra Red
WHO TDR	World Health Organization tropical disease research
PCR	polymerase chain reaction
PKDL	post-kala-azar dermal leshmaniasis
KDNA	kinetoplastic DNA
TEM	transmission electron microscopy
AFM	atomic force microscopy
ECM	extracellular matrix
HA	hydroxyapatite
PEVA	poly (ethylene-co-vinyl acetate)
PLA	Poly (lactic acid)
PLAGA	Poly (lactic acid co glycolic acid)
PA	Poly (tetra ethylene adipamine)
AMB	Amphotericin B
UV-Vis	Ultraviolet Visible
PCL	Polycaprolactone
TCD	Tip to collector distance

EXECUTIVE SUMMARY

Electrospun nanofibers were developed as a new system for the delivery of a medical drug amphotericin B. In this study drug loaded nanofibers of average diameter of 100nm were fabricated from a natural biodegradable polymer based on gelatin by advanced electrospinning process. The fibers in our research were prepared from 10 wt. % gelatin in acetic acid and water mixed with 1 wt. % amphotericin B and characterized by the Field Emission Scanning Electron Microscopy (FE-SEM) for observation of fiber morphology. The chemical integrity of the drug in electrospun nanofibers were confirmed by Fourier Transformation Infra Red (FTIR) spectroscopic analysis and the release of the amphotericin B from the electrospun fibers were further investigated by UV-Vis spectrophotometer in phosphate buffer of PH 7.4 at normal body temperature of 37°C. The release profile suggests that electrospun amphotericin B loaded biodegradable micro and nanofibers may be promising for the treatment of leishmaniasis and several severe fungal infections as alternative drug delivery devices.

Chapter 1

Introduction

Human visceral leishmaniasis also called Kala-Azar (KA), caused by *Leishmania donovani* complex, is a disseminated infection of spleen, liver, lymph nodes, bone marrow and other organs, and is fatal if it remains untreated [1]. The leishmaniasis afflicts the world's poorest populations. Among the two million new cases each year in the 88 countries where the disease is endemic, it is estimated that 80% people earn less than \$2 per day [2]. *Leishmania*, a unicellular trypanosomatid protozoan parasite causes a wide range of human diseases ranging from the localized self-healing cutaneous lesions to fatal visceral infections. *Leishmania* have a digenic life cycle, which is characterized by the presence of a flagellated promastigote form in the sand fly vector and a non motile amastigote stage within phagolysosomes of mammalian macrophages. It has been reported that visceral leishmaniasis (VL) in adult patients are co-infected with HIV from 33 countries [3]. Resistance to **pentavalent antimonials** [Sb (V)] has been reported earlier even from India which has been the first line of drug of choice for treatment of leishmaniasis [4-6]. Second line drugs e.g. **pentamidine** and **amphotericin B** has severe side effects and high cost, which limit their use despite of being a highly effective for this disease [7]. **Miltefosine** (hexadecylphosphocholine) has been approved as the first oral drug for leishmaniasis. It can be used for both antimony-sensitive and antimony-resistant patients [6]. In vitro studies have indicated that a single point mutation may lead to miltefosine resistant in the parasite and miltefosine is contra-indicated in pregnancy [8, 9].

Therefore, the treatment of drug resistant patients is a major problem which insists to find out new therapeutic targets against visceral leishmaniasis [10]. But at the same time, finding a therapeutically effective potent lead molecule through the current method of drug discovery is a lengthy process. The current technological advancement encourages us to find out an alternative strategy over such problems than to find out a potent lead molecule through the existing process of drug discovery. One of the current attractive approaches is development of a novel drug delivery system (DDS) which provide positive attributes to a

free drug by improving solubility, in vivo stability and biodistribution. These can also alter unfavorable pharmacokinetics of some free drugs. Moreover huge loading of pharmaceuticals on DDS can render drug reservoirs for controlled and sustained release to maintain the drug level within therapeutic window and thus improve the efficacy of the drug in larger folds. However, after 35 years of research in this field, AmBisome® (Amphotericin B liposome for injection, Astellas Pharma US, Inc.) is the only DDS used against the VL [11]. Hence it is very much important to increase the safety efficacy ratio of some important and highly suitable existing therapeutic by delivering through suitable delivery vehicles.

In recent years there is increased interest towards developing a suitable delivery system for several medical drugs by using polymeric materials in the form of nano or micro particles, hydrogels, micelles etc. Although those polymeric drug delivery materials have improved the therapeutic efficacy of medical drugs and reduced the side effects, there is still a need to address how to precisely control the drug releasing rate. Based on such background, people have recently focused on the usage of polymeric nanofibers which can encapsulate medical drugs instead of conventional polymeric materials. [12-21]. The main advantages of the fibrous carrier are that they offer site specific delivery of the drug to the body. Also more than one drug can be encapsulated directly into the fibers. Electrospinning is a simple and versatile technique capable of generating continuous fibers directly from a wide range polymers and composite materials. Due to the high surface area and porous structure of the electrospun fibers, they find the applications in many fields such as medicine, biosensors, catalysts, photonics, sensitized solar cells, tissue engineering, nanocomposites, antimicrobial materials and membranes [21]. Electrospinning technique is newly utilized in the field of drug delivery [12-21].

Considering the problems of curing leishmaniasis, in this study it is aimed to develop an efficient drug delivery system for the drug amphotericin B, which might be highly useful for the leishmaniasis patients.

Here, in this work it is proposed “electrospun polymeric nanofibers” as a new system for the delivery of the medical drug amphotericin B. The drug is a highly effective antileishmanial therapeutic [7]. Amphotericin B, an antifungal antibiotic were

used for controlling severe fungal infections and the same was also used as a potential therapeutic agent for the visceral leishmaniasis (**Kala-Azar**). Though amphotericin B is a highly effective kind of therapeutic agent against these diseases, one of its major drawbacks such as severe side effect limits its use since last several years. The proposed drug delivery systems (polymeric nanofibers) should allow the adverse effects caused by problematic routes of administration to be avoided as well as enhance the antileishmanial activity and reduce the toxicity of medication.

Gelatin is a natural biodegradable polymer having high degree of biocompatibility. Biodegradable polymers are good candidates for the application in the biomedical field due to their biocompatibility, their degradation and mechanical properties. Gelatin is derived from collagens and has almost identical compositions and biological properties as those of collagens. It is an aqueous polymer and has an important merit that it is a cheap biopolymer. By some post treatment or mixed with another (synthetic) biodegradable polymer[22], gelatin can be used alone or as a blend component to prepare nanofibrous membranes for tissue engineering scaffolds, wound healing, health caring devices and other biomedical applications.

In this work, the amphotericin B loaded natural biodegradable gelatin-nanofibers were fabricated by advanced electrospinning process, and the drug loaded fibers were characterized by the Scanning Electron Microscopy (**SEM**) for the study of fiber morphology. The electrospinning parameters were optimized to get the fibers with low diameter and best morphology. The chemical integrity of the drug in the drug loaded nanofiber was further confirmed by **FTIR** spectroscopic analysis. The release of amphotericin B from the drug loaded fibers was followed by **UV-Vis** spectroscopy in phosphate buffer at physiological pH and temperature

Chapter 2

Literature review

2.1 Introduction to leishmaniasis

Leshmaniasis remains a major public health problem today despite the vast amount of research conducted on *Leishmania* pathogens. The parasitic protozoa of the genus *Leishmania* Ross, 1903 are the pathogenic agents responsible for leshmaniasis [23]. In humans, the disease occurs in at least four major forms: cutaneous, diffuse cutaneous, mucocutaneous, and viscera [24, 25]. Cutaneous leshmaniasis is frequently self-healing in the 'Old World' but, when the lesions are multiple and disabling with disfiguring scars, it creates a lifelong aesthetic stigma. It's most severe form, recidivans leshmaniasis, is very difficult to treat, long-lasting, destructive and disfiguring. Diffuse cutaneous leshmaniasis occurs in individuals with a defective cell-mediated immune response.

In 2002, the WHO estimated the number of persons at risk to be around 350 million and the number of new cases to be 23, 57,000 per year. In India about 1, 00,000 cases of visceral leshmaniasis (VL) are estimated to occur annually; of these, the State of Bihar accounts for over than 90 % of the cases. Nevertheless, these diseases are still considered as neglected diseases. For all these reasons, research on these parasites is necessary to improve diagnosis and hence epidemiological study and also to support drug and vaccine development. Furthermore, *Leishmania spp.* can produce a great variety of clinical symptoms in humans. The genetic determinants responsible for this clinical polymorphism are still unknown, making this biological model complex from ecological, genetic and phylogenetic points of view [23].

Most of *Leishmania* infections are zoonotic and rodents and candidids are reservoir host. Only two *Leishmania* species can maintain anthroponotic, human-human cycle, these species are *L.donovani* responsible for VL in Indian subcontinent and east Africa and *L. tropica*, which is responsible for cutaneous leshmaniasis (CL) in the Old World. The different epidemiological cycles are (i) a primitive or sylvatic cycle (human infection is

accidental, transmission occurring in wild foci), e.g. *L. braziliensis*; (ii) a secondary or peridomestic cycle (the reservoir is a peridomestic or domestic animal, the parasite being transmitted to humans by anthropophilic sand flies), e.g. *L. infantum*; and (iii) a tertiary, strictly anthroponotic cycle, in which the animal reservoir has disappeared (or not yet been identified) and the sand fly vectors are totally anthroponotic, e.g. *L. donovani* [23].

Leshmaniasis has been considered a tropical affliction that constitutes one of the six entities on the World Health Organization tropical disease research (WHO TDR) list of most important diseases [24]. It occurs in 88 countries in tropical and temperate regions, 72 of them developing or least developed [25].

Indian VL (Kala-azar, Black fever), caused by *L. donovani*, is the systemic form of disease. The risk of VL among AIDS patients increases by 100-1000 times in endemic areas; while VL accelerates the onset of AIDS in HIV infected people [26].

2.1.1 Life cycle

During their complex life cycle (Figure 2.2), *Leishmania* parasites are exposed to different extra- and intracellular environments. These organisms are digenetic parasites with two basic life cycle stages: one extracellular stage within an invertebrate host (*phlebotomine* sand fly) and one intracellular stage within a vertebrate host. Thus, the parasites exist in two main morphological forms, amastigotes and promastigotes, (Figure 2.1) which are found in vertebrate hosts and invertebrate hosts, respectively [23].

2.1.1.1 Stages in invertebrate host

The invertebrate hosts or vectors are small insects of the order *Diptera*, belonging to the subfamily *Phlebotominae*. They are commonly called *phlebotomine* sand flies. Of the six genera described, only two are of medical importance: *Phlebotomus* of the 'Old World', and *Lutzomyia* of the 'New World'. All known vectors of the leshmaniasis are species of these two genera. Within the intermediate host, *Leishmania* develops as promastigote forms, elongated motile extracellular stages possessing a prominent free flagellum

2.1.1.2 Stages in vertebrate host

Leishmania are extremely successful parasites and natural infections are found in many different orders of mammals [27]. Humans are possible hosts of these parasites, but in the majority of cases they are considered to be accidental hosts. Although susceptible to infection with many *Leishmania* species whose natural hosts range from edentates to rodents [28], humans are not bitten regularly by the vector and they are not involved in the enzootic cycle. In the vertebrate host, the parasite evolves into an amastigote form. Amastigotes are ovoid (2.5–5 μm diameter), nonmotile intracellular stages. They do not have a free flagellum and are located in the parasitophorous vacuoles of the host's macrophages.

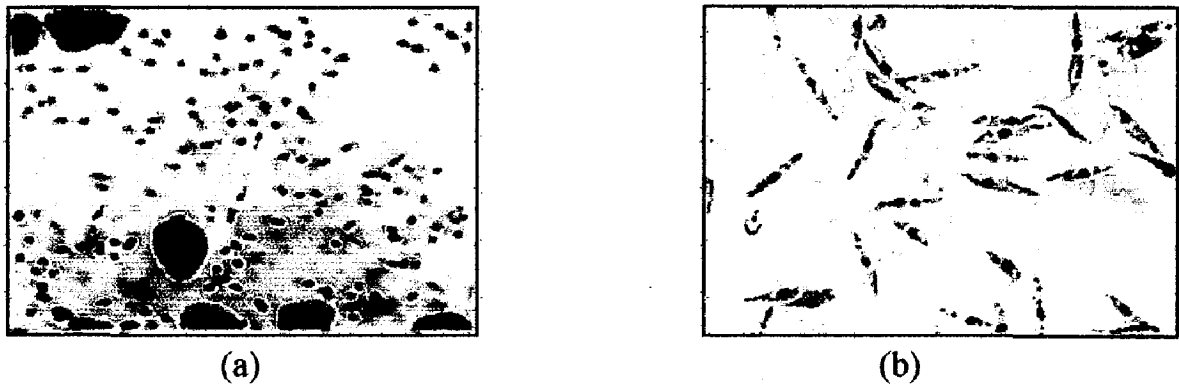


Fig: 2.1 *Leishmania infantum* (a) Amastigote (b) Promastigote

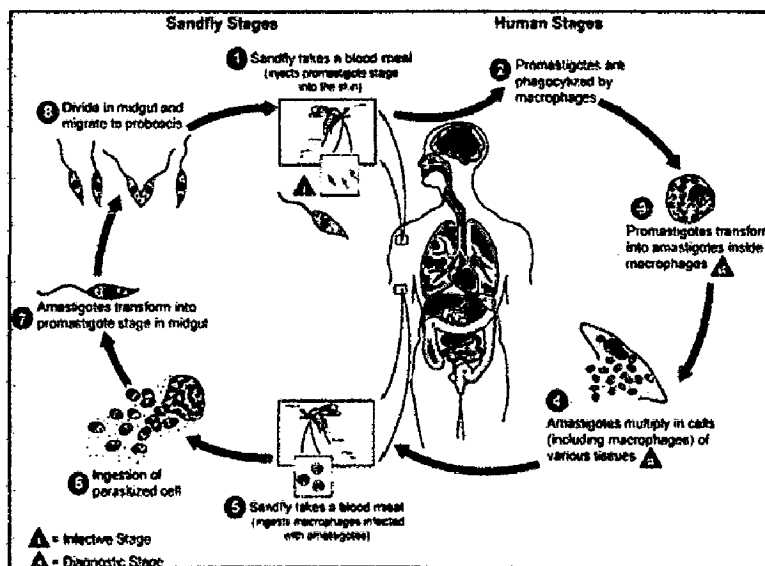


Fig: 2.2 Life cycle of leishmaniasis [47]

2.1.2 Clinical diversity in human

The hypothesis, based on epidemiological data, is that the majority of *Leishmania* species are adapted to a large range of hosts, and that the infections remain asymptomatic. On the other hand, in animals that are less well adapted, such as humans, infections can produce a wide range of diversified pathologies, from asymptomatic carriers and benign cutaneous lesions to more serious cases such as the visceral form. When humans are bitten by an infective sand fly, parasite inoculation can lead to the development of leishmaniasis but can also have no effect on health. The rate of asymptomatic carriers (infected individuals without clinical manifestations) is not accurately known, but different studies have suggested that it may be higher than expected. For example, in the Balearic Islands, *L. infantum* DNA was amplified by the polymerase chain reaction (PCR) from the blood of 22% of donors [29] and asymptomatic carriers have also been identified in Brazil, southern France and India.

Mucocutaneous leishmaniasis, also known as espundia, causes extensive destruction of oro-nasal and pharyngeal cavities with hideously disfiguring lesions, mutilation of the face and great life-long distress for the patient. Visceral leishmaniasis, also known as kala-azar, is the most severe form (nearly always fatal if left untreated), characterized by undulating fever, loss of weight, splenomegaly, hepatomegaly and/or lymphadenopathies and anemia. After recovery, patients may develop a chronic cutaneous form called post-kala-azar dermal leishmaniasis (PKDL), which usually requires long and expensive treatment [6].

2.1.3 Taxonomy

The classification of *Leishmania* (Figure 2.3) was initially based on ecobiological criteria such as vectors, geographical distribution, tropism, antigenic properties and clinical manifestation. However, biochemical and molecular analysis showed that pathological and geographical criteria were often inadequate and thus other criteria such as the patterns of polymorphism exhibited by kinetoplastic DNA (kDNA) markers, proteins or antigens came to be used to classify *Leishmania* [6]. All members of the genus *Leishmania* Ross, 1903 are parasites of mammals. The two subgenera, *Leishmania* and *Viannia*, are separated on the basis of their location in the vector's intestine [27].

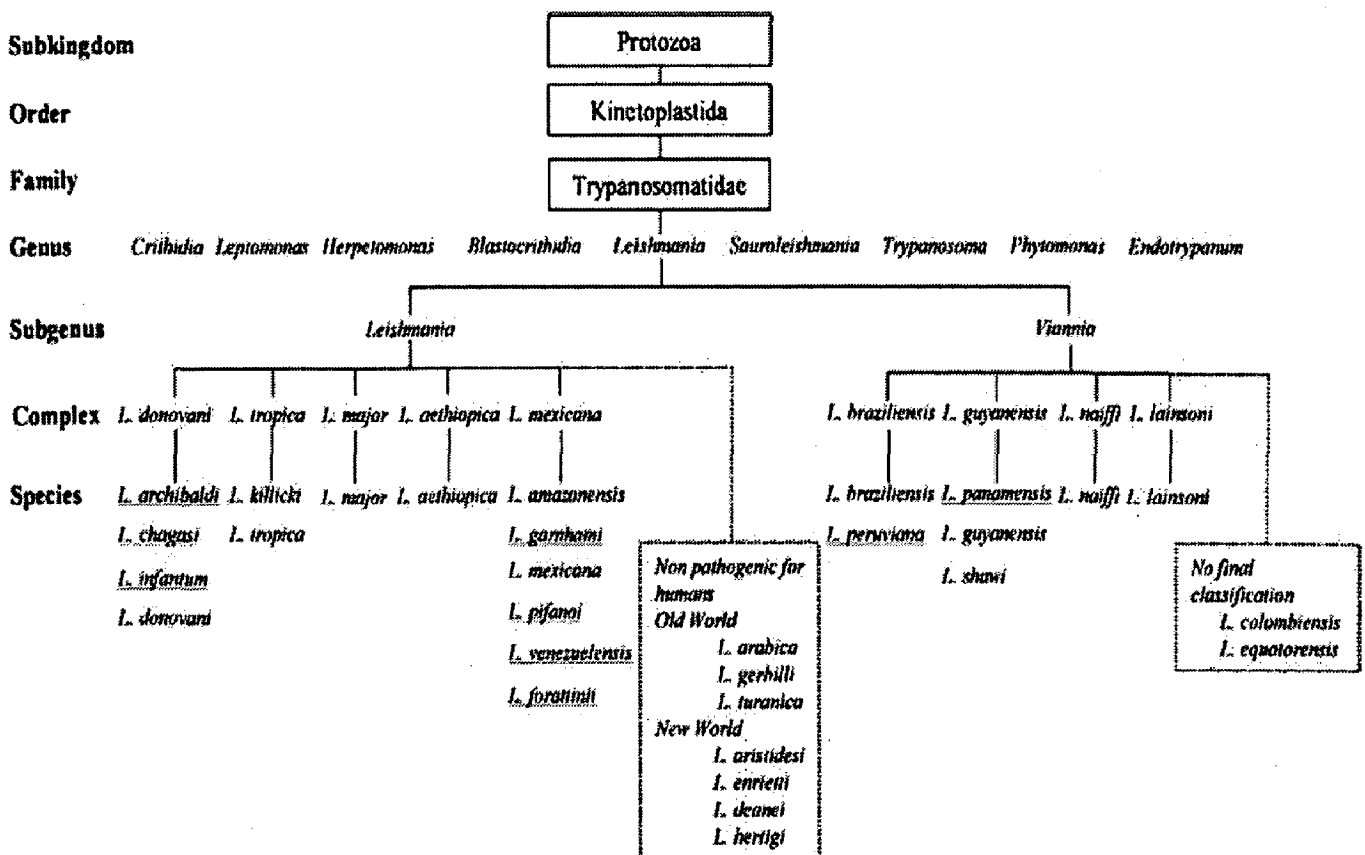


Fig: 2.3 Taxonomy of *Leishmania sp* [23].

These species generally present different epidemiological and clinical characteristics related to different genetic and phenotypic profiles.

2.1.4 Symptoms

Systemic visceral infection in children usually begins suddenly with vomiting, diarrhea, fever, and cough. Adults usually have a fever for 2 weeks to 2 months, along with nonspecific symptoms such as fatigue, weakness, and loss of appetite. Weakness increases as the disease gets worse [30].

Other symptoms of systemic visceral leishmaniasis may include:

- Cough (children)
- Diarrhea (children)
- Fever that persists for weeks; may come and go in cycles
- Night sweats
- Scaly, gray, dark, ashen skin

- Thinning hair
- Vague belly area (abdominal) discomfort
- Vomiting (children)
- Weight loss

2.1.5 Treatment

Medicines called antimony-containing compounds are the main drugs used to treat leishmaniasis. These include:

- Meglumine antimonate
- Sodium stibogluconate

Other drugs that may be used include:

- Amphotericin B
- Pentamidine

Plastic surgery may be needed to correct disfigurement by destructive facial lesions (cutaneous leishmaniasis). Removal of the spleen (splenectomy) may be required in drug-resistant cases of visceral leishmaniasis.

2.2 Electrospinning and nanofiber

Electro-spinning is a remarkably simple and versatile technique capable of generating continuous fibers directly from a wide range polymers and composite materials. It is useful for production of fibers in the range of tens of nanometers to micrometers, and the fibers can be deposited as nonwoven mats, or aligned into uniaxial arrays and further stacked into multilayered architectures. This technique was demonstrated more than 100 years ago and was first patented in the 1930s [31]. Polymer nanofibers exhibit several properties that make them favorable for many applications. Nanofibers have a very large surface area to volume ratio, flexibility in surface functionalities, and mechanical properties superior to larger fibers. Nanofibers have increasingly found their way into a broad range of nonwovens applications such as medical barriers, protective garments, face masks, cosmetics, hygiene, acoustic and thermal insulation, battery separators, tissue scaffolds, and even fashion. Because of the simple method of production and wide scope of applicability of nanofibers, scientists and engineers are giving tremendous efforts for its research and development for their commercial applications, and research papers in the

area of nanofibers have been increasing exponentially. It will be discussed here about the fabrication of nanofibers by electrospinning, mechanism of fiber formation, process optimization (production controlling parameters), and applications of nanofibers.

2.2.1 Experimental set up

Electrospinning is a technique by which nanoscale polymeric fibers can be fabricated by subjecting a polymer solution to an electric field. Electro-spinning begins with a polymer solution loaded in a syringe fitted with a capillary needle is applied to solution within the capillary, usually via an electrode. An electric field mounted inside the needle which is connected to a high voltage power source [1KV-50KV]. As the electric field increases, a charge builds at the tip of the capillary and develops into a repulsive force which eventually exceeds the force of the polymer's surface tension and a charged jet of polymer solution is emitted from the capillary. As the jet leaves the tip,

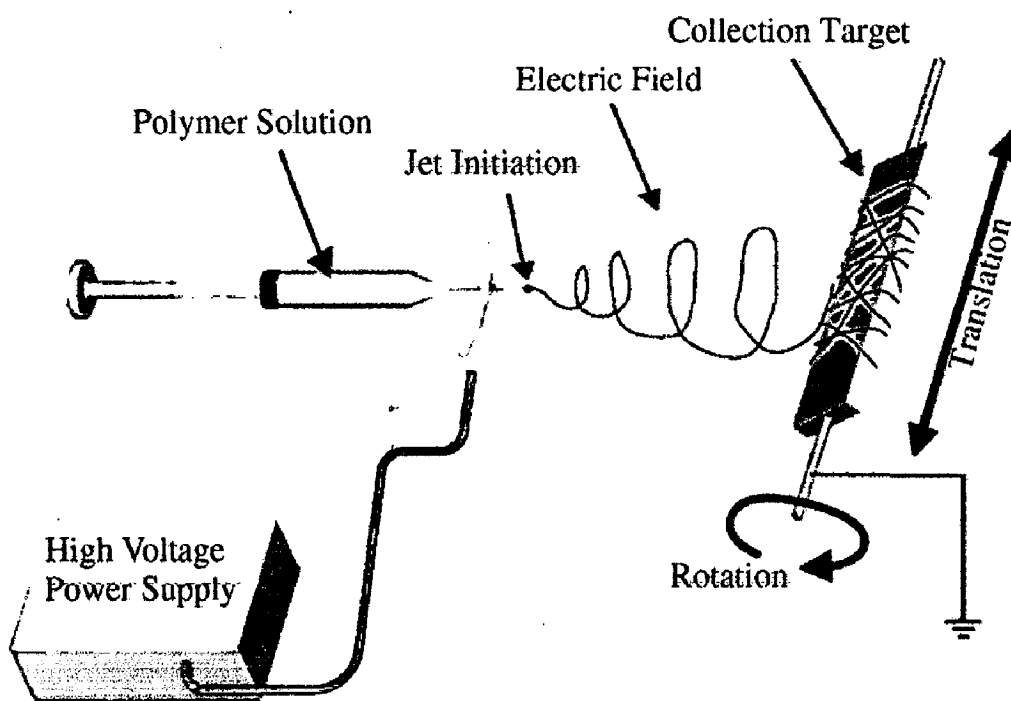


Fig: 2.4 *Generic electro-spinning set-up depicting the major components of the electro-spinning process, including a high-voltage power supply, polymer solution and grounded collection target. [Source: Polymer Int 56: 1349–1360 (2007)]*

it thins considerably and it may experience a fluid instability resulting in bending of the jet and even whip-like motion. Since the charge on this jet allows its path to be guided by an electric field, a metal screen is often used to collect the charged polymer fiber that forms when the solvent evaporates from the polymer jet. This fiber deposits itself randomly as it contacts the screen,

forming a non-woven material. Electrospinning may be used to create fibers with diameters ranging from 50 nm to 5 μm . Electrospinning has been used to fabricate nanofiber meshes from a variety of polymers depending on applications.

2.2.2 Physics of fiber formation

Although the setup for electro-spinning is incredibly simple, the mechanism of spinning fibers under the influence of an electric field is rather complicated. The essence of electro-spinning is to generate a continuous jet by immobilizing charges onto the surface of a pendent droplet. In order to better understand the basic aspects, an electro-spinning process can be divided into five major steps: i) charging of the pendent droplet; ii) formation of the cone-jet otherwise called Taylor cone; iii) thinning of the steady jet; iv) onset and growth of jet stabilities that give rise to a diameter reduction into nanometer-scale sizes; and v) collection of the fibers in different forms [32]. It has recently been resolved that the spinning process is mainly driven by whipping rather than splaying of a jet. [33, 34] Figure 2.5 shows a typical electro-spinning jet captured using a high-speed camera [35]. The whipping instability originates from the electrostatic interactions between

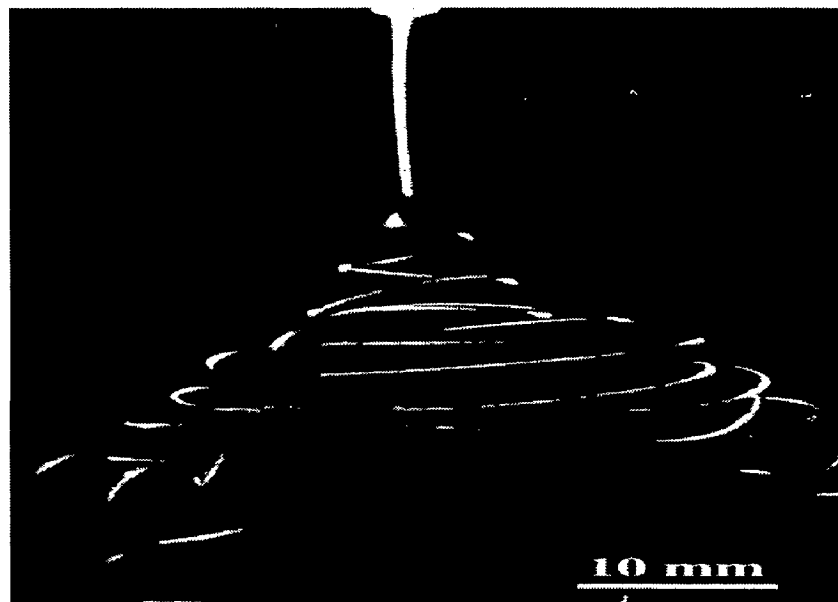


Fig: 2.5 Photographs of typical electrospinning jets captured using a high-speed camera showing the electrically driven bending instability. (Courtesy reference [5], copyright 2007 Elsevier.)

the external electric field and the surface charges on the jet. Formation of fibers with nanometer-scale diameters is achieved by stretching and acceleration of the unstable fluid filament until it has been solidified or it has been deposited on the collector. The liquid jet has to maintain a suitable viscoelasticity in order to survive the whipping process. A jet can occasionally split into two jets that splay apart, with the axis of the thinner branch being positioned perpendicular to the primary jet. In addition to experimental investigations, mathematical models have been developed to gain insight into the electro-spinning process for a better understanding of the mechanistic details involved in this process, which has been used to guide the optimal design of new setups and to achieve a better control over the size, alignment, and assembly of the electro-spun fibers [33-38].

2.2.3. Process optimization

2.2.3.1 Processing parameters

The basic processing parameters include applied voltage, polymer flow rate, and capillary-collector distance.

2.2.3.1.1 Applied voltage

The strength of the applied electric field controls formation of fibers from several microns in diameter to tens of nanometers. Suboptimal field strength could lead to bead defects in the spun fibers or even failure in jet formation [39]. Deitzel et al. examined a polyethylene oxide (PEO)/water system and found that increases in applied voltage altered the shape of the surface at which the Taylor cone and fiber jet were formed [40]. At lower applied voltages the Taylor cone formed at the tip of the pendent drop; however, as the applied voltage was increased the volume of the drop decreased until the Taylor cone was formed at the tip of the capillary, which was associated with an increase in bead defects seen among the electrospun fibers it is evident that there is an optimal range of electric field strengths for a certain polymer/solvent system, as either too weak or too strong a field will lead to the formation of beaded fibers.[39]

2.2.3.1.2 Flow rate

Polymer flow rate also has an impact on fiber size, and additionally can influence fiber porosity as well as fiber shape. Both fiber diameter and pore size increase with

increasing flow rate. At high flow rates significant amounts of bead defects were noticeable, due to the inability of fibers to dry completely before reaching the collector. Incomplete fiber drying also leads to the formation of ribbon like (or flattened) fibers as compared to fibers with a circular cross section. [39]

2.2.3.1.3 Capillary to collector distance

The distance between capillary tip and collector can also influence fiber size by 1-2 orders of magnitude. Sufficient distance should be maintained in order to dry the solvent completely so as to get the nanofibers, otherwise bead formation become predominant upon shortening of the distance between the capillary tip and the collector, which can be attributed to inadequate drying of the polymer fiber prior to reaching the collector.[39]

2.2.3.2 Solution parameters

In addition to the processing parameters a number of solution parameters play an important role in fiber formation and structure. In relative order of their impact on the electro-spinning process these include polymer concentration, solvent volatility and solvent conductivity. [39]

2.2.3.2.1 Polymer concentration

The polymer concentration determines the spin ability of a solution, namely whether a fiber forms or not. The solution must have a high enough polymer concentration for chain entanglements to occur; however, the solution cannot be either too dilute or too concentrated. The polymer concentration influences both the viscosity and the surface tension of the solution, both of which are very important parameters in the electro-spinning process. If the solution is too dilute then the polymer fiber will break up into droplets before reaching the collector due to the effects of surface tension. However, if the solution is too concentrated then fibers cannot be formed due to the high viscosity, which makes it difficult to control the solution flow rate through the capillary. Thus, an optimum range of polymer concentrations exists in which fibers can be electrospun when all other parameters are held constant. In many experiments it has been shown that within the optimal range of polymer concentrations fiber diameter increases with increasing polymer concentration [39].

2.2.3.2.2 Solvent volatility

Choice of solvent is also critical as to whether fibers are capable of forming, as well as influencing fiber porosity. In order for sufficient solvent evaporation to occur between the capillary tip and the collector a volatile solvent must be used. As the fiber jet travels through the atmosphere toward the collector a phase separation occurs before the solid polymer fibers are deposited, a process that is greatly influenced by the volatility of the solvent. It is found that more volatile solvent tend to increase the fibers of high pore density and less volatile solvent tend to yield fibers with low pore density.[39]

2.2.3.2.3 Solution conductivity

Solution conductivity can influence fiber size within 1 to 2 orders of magnitude. Solutions with high conductivity will have a greater charge carrying capacity than solutions with low conductivity. Thus the fiber jet of highly conductive solutions will be subjected to a greater tensile force in the presence of an electric field than will a fiber jet from a solution with a low conductivity. So highly conductive solution can capable of producing lesser diameter nanofibers. Similarly addition of little amount of salts such as NaCl causes the decrease in the mean fiber diameter of fibers due to increased net charge density imparted by the salt, which increased the electric force exerted on the jet. [39]

2.2.3.3 Ambient parameters

These parameters include environmental temperature and humidity. This affects the electro-spinning by producing spark in the electrical connection as it is operated at very high voltage which causes energy loss.

2.2.4. Characterization of nanofibers

Geometric properties of nanofibers such as fiber diameter, diameter distribution, fiber orientation and fiber morphology (e.g. cross-section shape and surface roughness) can be characterized using scanning electron microscopy (SEM), field emission scanning electron microscopy (FESEM), transmission electron microscopy (TEM) and atomic force microscopy (AFM). The use of TEM does not require the sample in a dry state as that of SEM. Hence, nanofibers electro-spun from a polymer solution can be directly observed

under TEM. Fig. 2.6 shows the nanofiber structures observed through SEM, TEM and AFM. [41]

Both the individual nanofibers and the webs formed from the nanofibers require accurate measurement and description in terms of their diameter, uniformity, length, web thickness, web structure, web size, fiber packing density, and production speed.

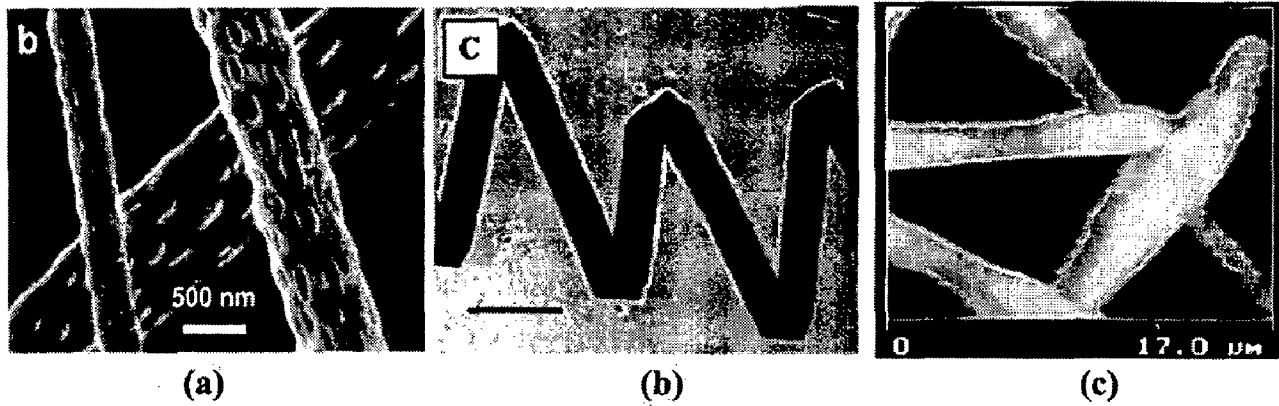


Fig: 2.6 (a) SEM of PLLA nanofibers ([41]), (b) TEM of elastin-mimetic peptide fibers (bar represents 3.3 mm) ([41]), and (c) AFM of polyurethane nanofibers ([41])

2.2.5 Potential applications

Electro-spinning is a remarkably simple and powerful technique for generating ultrathin fibers from a wealth of different materials. The simplicity of the fabrication scheme, the diversity of the material suitable for use with electro-spinning as well as the unique and interesting features associated with electro-spun nanofibers, all make this technique and resultant structures attractive for number of applications such as tissue engineering scaffolds, filtration devices, sensors, materials development, electronic applications etc. Some of the important applications are briefly described below.

2.2.5.1 Nanofiber reinforced composites

Fiber based reinforcement represents one of the most effective strategies for enhancing the strength and other performance of a composite material. Because of the high surface to volume ratio, use of the nanofibers as components may significantly increase the interaction between the fibers and matrix material, leading to better reinforcement than conventional fibers [42].

2.2.5.2 Nanofiber based membranes and smart cloths

The extreme porosity of nanofiber mats make it higher convective resistance to air flow compared to normal clothing materials while the resistance to transport of water vapor was much lower than commercial membrane laminates. In particular the electro-spun membrane exhibited the excellent ability to capture the aerosol particles. The filtration efficiency was also high even though an extremely thin layer of electro-spun fibers was used. The light weight breathable mats made up of electro-spun nanofibers are promising candidates for applications such as protective clothing. With the incorporation of magnetic components, it is expected that the separation efficiency for magnetic active particles can be further enhanced through the application of an external magnetic field. In principle, it is possible to incorporate many type of active components and species into electrospun nanofibers to fabricate smart clothes that are responsive to all the changes in surrounding [42].

2.2.5.3 Biomedical applications

As such, current research in electro-spun polymer nanofibers has focused one of their major applications on bioengineering. We can easily find their promising potential in various biomedical areas. Some examples are listed as below.

2.2.5.3.1 Tissue engineering

For the treatment of tissues or organs in malfunction in a human body, one of the challenges to the field of tissue engineering/biomaterials is the design of ideal scaffolds/synthetic matrices that can mimic the structure and biological functions of the natural extracellular matrix (ECM) —a 3D network of collagen fibers 50–500 nm in diameter. Non-woven mats of electro-spun nanofibers can serve as ideal scaffolds for tissue engineering because they can mimic the extracellular matrix (ECM) in that the architecture of nanofibers is similar to the collagen structure of the ECM. Furthermore, electro-spun nanofibers have several advantages for tissue regeneration: desirable topography (e.g., 3D porosity, nanometer-scale size, and alignment), encapsulation and local sustained release of growth factors, and surface functionalization (e.g., surface immobilization of bioactive molecules or functional groups). Scaffold materials used for tissue engineering have to be biocompatible and notable examples include natural or

synthetic biodegradable polymers, biocompatible polymers, and composites with bioactive inorganic solids such as hydroxyapatite (HA) [42].

2.2.5.3.2 Encapsulation of bioactive materials

Encapsulation of bioactive materials is usually used to functionalize electro-spun fibers for various applications (e.g. sustained delivery of therapeutic agents, immobilization of bioactive species, and release of growth factors for enhancement of cells proliferation and functions). For encapsulation of bioactive species in polymeric fibers, a simple mixture of oil and water phases or a water/oil emulsion is usually used as long as one can achieve a uniform distribution for the materials loaded into the nanofibers. The bioactivity of bio-macromolecules has to be carefully examined during this process due to their tendency to denature and thus lose the function. For e.g. Wnek and co-workers pioneered the use of electro-spinning to encapsulate tetracycline hydrochloride (used as a model drug) inside electro-spun fibers of poly (ethylene-co-vinyl acetate) (PEVA), poly(lactic acid) (PLA), and a blend of these polymers, and then examined the release of the drug from the fibers.[43]. Similarly an anticancer drug-paclitaxel loaded PLGA nanofibers were fabricated which can be used as implants for sustained delivery of paclitaxol for the treatment of C6 glioma in vitro[44].

2.2.5.3.3 Wound dressing

Polymer nanofibers can also be used for the treatment of wounds or burns of a human skin, as well as designed for haemostatic devices with some unique characteristics. With the aid of electric field, fine fibers of biodegradable polymers can be directly sprayed/spun onto the injured location of skin to form a fibrous mat dressing, which can let wounds heal by encouraging the formation of normal skin growth and eliminate the formation of scar tissue which would occur in a traditional treatment. On-woven nanofibrous membrane mats for wound dressing usually have pore sizes ranging from 500 nm to 1 mm, small enough to protect the wound from bacterial penetration via aerosol particle capturing mechanisms [42].

2.2.5.3.4 Medical prostheses

Polymer nanofibers fabricated via electro-spinning have been proposed for a number of soft tissue prostheses applications such as blood vessel, vascular, breast, etc. In addition, electro-spun biocompatible polymer nanofibers can also be deposited as a thin porous film onto a hard tissue prosthetic device designed to be implanted into the human body. This coating film with gradient fibrous structure works as an interphase between the prosthetic device and the host tissues, and is expected to efficiently reduce the stiffness mismatch at the tissue/device interphase and hence prevent the device failure after the implantation [42].

2.2.5.3.5 Cosmetics

The current skin care masks applied as topical creams, lotions or ointments may include dusts or liquid sprays which may be more likely than fibrous materials to migrate into sensitive areas of the body such as the nose and eyes where the skin mask is being applied to the face. Electro-spun polymer nanofibers have been attempted as a cosmetic skin care mask for the treatment of skin healing, skin cleansing, or other therapeutic or medical properties with or without various additives. This nanofibrous skin mask with very small interstices and high surface area can facilitate far greater utilization and speed up the rate of transfer of the additives to the skin for the fullest potential of the additive. The cosmetic skin mask from the electro-spun nanofibers can be applied gently and painlessly as well as directly to the three-dimensional topography of the skin to provide healing or care treatment to the skin [42].

2.2.5.4 Electrical and optical applications

Conductive nanofibers are expected to be used in the fabrication of tiny electronic devices or machines such as Schottky junctions, sensors and actuators. Due to the well-known fact that the rate of electrochemical reactions is proportional to the surface area of the electrode, conductive nanofibrous membranes are also quite suitable for using as porous electrode in developing high performance battery. Conductive (in terms of electrical, ionic and photoelectric) membranes also have potential for applications including electrostatic dissipation, corrosion protection, electromagnetic interference shielding, photovoltaic device, etc [42].

3.2 Characterization and spectroscopic techniques

The morphology of drug loaded gelatin dried fibers were investigated with a Field Emission Scanning Electron microscope (QUANTA 200F FEI, Netherlands). Fiber mats were sputtered with a thin layer of gold prior to SEM observation.

FTIR (THERMO NICOLET, NEXUS) is used for the confirmation of chemical integrity of the drug in amphotericin B loaded gelatin nanofibers obtained after electrospinning. Ultra visible spectra were recorded using a UV-Vis spectrophotometer (S/STRONICS 118) for the calibration curve preparation and monitoring the drug release.

3.3 Electrospinning

3.3.1 Preparation of drug loaded polymer solution

The dry powder of amphotericin B of 50mg was reconstituted by adding 10ml of sterile water. The concentration of amphotericin B was reached to 5mg/ml and was kept as stock at 4°C in refrigerator for further preparation of electrospinning polymer solution.

Required volume of stock amphotericin B (5mg/ml) was added to gelatin solution prepared by mixing different concentration (wt %) of gelatin (table 3.1) with acetic acid and water in the ratio 4:1 so that the amount of amphotericin B in the electrospinning solution would be 1 wt% (based on weight of the polymer gelatin). The obtained solution was subsequently sonicated with the help of a sonicator prior to electrospinning for uniform mixing of drug with polymer solution.

Table 3.1 shows the composition of different weight percentage of gelatin that were used for electrospinning to choose the best concentration range for drug loaded gelatin nanofibers preparation.

Table 3 1: *Different composition of gelatin, amphotericin B, acetic acid and water in the solution.*

S. No.	Gelatin concentration (wt %)	Total volume of electrospinning solution (ml)	Gelatin amount (gm)	Drug solution (ml)	Double distilled water (ml)	Acetic acid (ml)
1	8	5	0.40	0.8	0.2	4
2	9	5	0.45	0.9	0.1	4
3	10	5	0.50	1.0	0.0	4

2.2.5.3.4 Medical prostheses

Polymer nanofibers fabricated via electro-spinning have been proposed for a number of soft tissue prostheses applications such as blood vessel, vascular, breast, etc. In addition, electro-spun biocompatible polymer nanofibers can also be deposited as a thin porous film onto a hard tissue prosthetic device designed to be implanted into the human body. This coating film with gradient fibrous structure works as an *interphase* between the prosthetic device and the host tissues, and is expected to efficiently reduce the stiffness mismatch at the tissue/device interphase and hence prevent the device failure after the implantation [42].

2.2.5.3.5 Cosmetics

The current skin care masks applied as topical creams, lotions or ointments may include dusts or liquid sprays which may be more likely than fibrous materials to migrate into sensitive areas of the body such as the nose and eyes where the skin mask is being applied to the face. Electro-spun polymer nanofibers have been attempted as a cosmetic skin care mask for the treatment of skin healing, skin cleansing, or other therapeutic or medical properties with or without various additives. This nanofibrous skin mask with very small interstices and high surface area can facilitate far greater utilization and speed up the rate of transfer of the additives to the skin for the fullest potential of the additive. The cosmetic skin mask from the electro-spun nanofibers can be applied gently and painlessly as well as directly to the three-dimensional topography of the skin to provide healing or care treatment to the skin [42].

2.2.5.4 Electrical and optical applications

Conductive nanofibers are expected to be used in the fabrication of tiny electronic devices or machines such as Schottky junctions, sensors and actuators. Due to the well-known fact that the rate of electrochemical reactions is proportional to the surface area of the electrode, conductive nanofibrous membranes are also quite suitable for using as porous electrode in developing high performance battery. Conductive (in terms of electrical, ionic and photoelectric) membranes also have potential for applications including electrostatic dissipation, corrosion protection, electromagnetic interference shielding, photovoltaic device, etc [42].

2.2.5.5 Filtration application

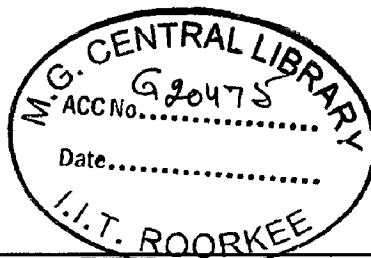
Filtration is necessary in many engineering fields. Fibrous materials used for filter media provide advantages of high filtration efficiency and low air resistance. Filtration efficiency, which is closely associated with the fiber fineness, is one of the most important concerns for the filter performance. It is realized that electro-spinning is rising to the challenge of providing solutions for the removal of unfriendly particles in such submicron range. In general, due to the very high surface area to volume ratio and resulting high surface cohesion, tiny particles of the order of <0.5 μm can be easily trapped in the electro-spun nanofibrous structured filters and hence the filtration efficiency can be improved [42].

2.2.5.6 Other functional applications

Nanofibers from polymers with piezoelectric effect will make the resultant nanofibrous devices piezoelectric for e.g. Polyvinylidene fluoride. Nanofibers from such polymers could be used in developing functional sensors with sensitivity. Nanofiber films can be employed as a new sensing interface for developing chemical and biochemical sensor applications for e.g. Poly (lactic acid co glycolic acid) (PLGA). Similarly highly sensitive optical sensors based on fluorescent electro-spun polymer nanofiber films were also recently reported. Ultrafine fibers prepared from electro-spinning can be used as templates to develop the various nanotubes. For e.g. PA [poly (tetra ethylene adipamide)] and PLA nanofibers of smaller diameter can be used as templates for the construction of thinner nanotubes [42].

Chapter 3

Experimental



3.1 Materials

Gelatin Type-A (low molecular weight) & acetic acid were purchased from M/S Sigma Aldrich, Germany. Phosphate Buffer Saline (PBS) without calcium and magnesium was purchased from M/S Himedia Laboratories India Limited. Amphotericin B was purchased from M/S Nicholas Primal (India) Limited. The chemical structures of polymer gelatin & drug amphotericin B are shown in fig 3.1. All these materials were used as received without further purification.

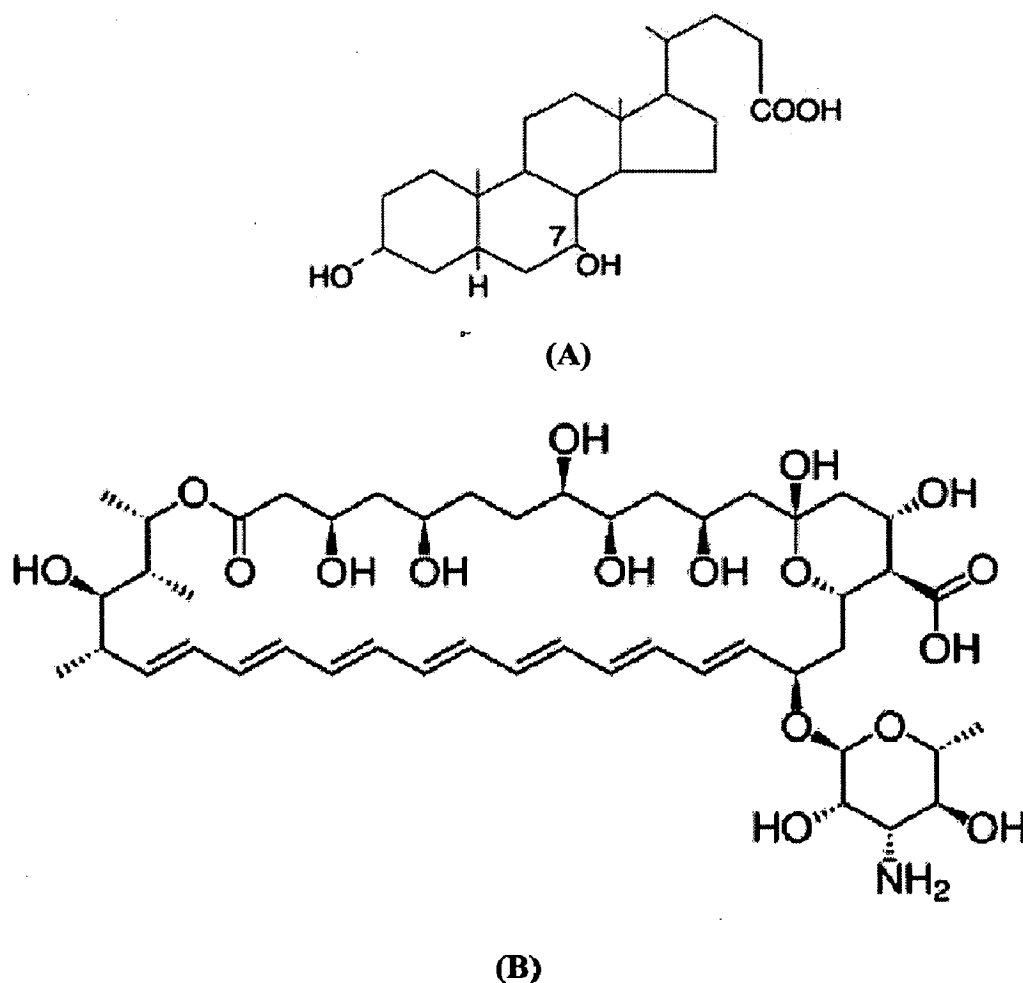


Fig: 3.1 Chemical Structure of (A) Gelatin and [45], (B) Amphotericin B [46]

3.2 Characterization and spectroscopic techniques

The morphology of drug loaded gelatin dried fibers were investigated with a Field Emission Scanning Electron microscope (QUANTA 200F FEI, Netherlands). Fiber mats were sputtered with a thin layer of gold prior to SEM observation.

FTIR (THERMO NICOLET, NEXUS) is used for the confirmation of chemical integrity of the drug in amphotericin B loaded gelatin nanofibers obtained after electrospinning. Ultra visible spectra were recorded using a UV-Vis spectrophotometer (S/STRONICS 118) for the calibration curve preparation and monitoring the drug release.

3.3 Electrospinning

3.3.1 Preparation of drug loaded polymer solution

The dry powder of amphotericin B of 50mg was reconstituted by adding 10ml of sterile water. The concentration of amphotericin B was reached to 5mg/ml and was kept as stock at 4°C in refrigerator for further preparation of electrospinning polymer solution.

Required volume of stock amphotericin B (5mg/ml) was added to gelatin solution prepared by mixing different concentration (wt %) of gelatin (table 3.1) with acetic acid and water in the ratio 4:1 so that the amount of amphotericin B in the electrospinning solution would be 1 wt% (based on weight of the polymer gelatin). The obtained solution was subsequently sonicated with the help of a sonicator prior to electrospinning for uniform mixing of drug with polymer solution.

Table 3.1 shows the composition of different weight percentage of gelatin that were used for electrospinning to choose the best concentration range for drug loaded gelatin nanofibers preparation.

Table 3 1: *Different composition of gelatin, amphotericin B, acetic acid and water in the solution.*

S. No.	Gelatin concentration (wt %)	Total volume of electrospinning solution (ml)	Gelatin amount (gm)	Drug solution (ml)	Double distilled water (ml)	Acetic acid (ml)
1	8	5	0.40	0.8	0.2	4
2	9	5	0.45	0.9	0.1	4
3	10	5	0.50	1.0	0.0	4

3.3.2 General procedure for electrospinning

The electrospinning was done with the help of an electrospinning apparatus equipped with a syringe having flat-end metal needle cut, a syringe pump (Model 11 Plus, Harvard Apparatus) for controlling feeding rate and a high voltage DC power supply for injecting charge to polymer droplet. The solution was placed in a syringe; positive or negative voltage was applied to initiate jet. The feeding rate was controlled by the syringe pump and the tip to collector distance (TCD) was adjusted. The figure 3.2 shows a typical electrospinning instrument that *has been used for this work*.

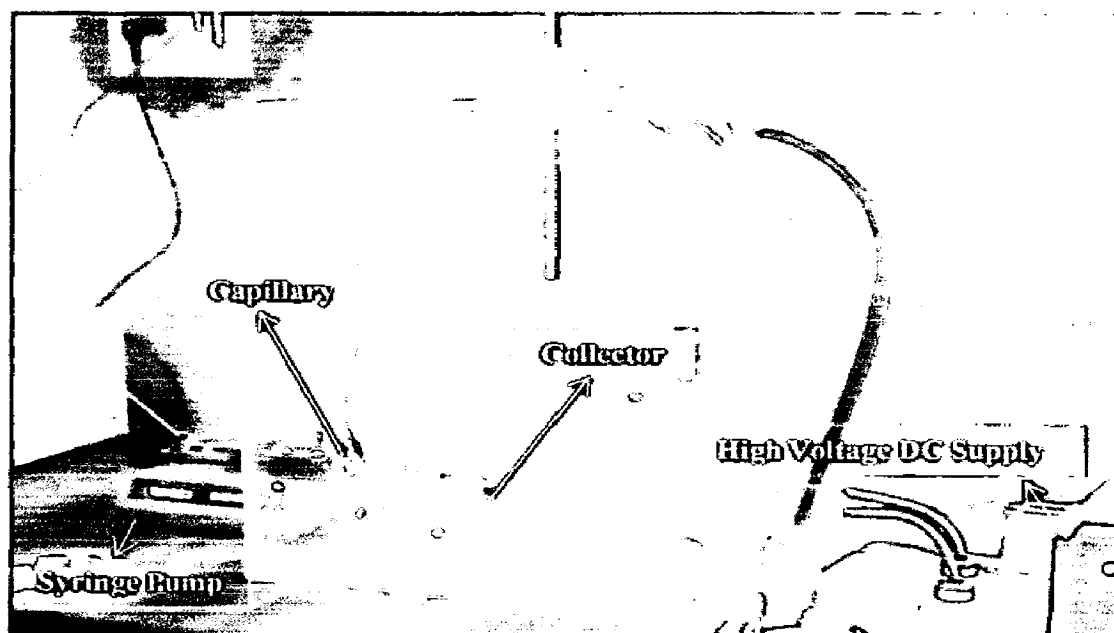


Fig 3.2: Electrospinning instrument of Tissue Engineering Laboratory, Department of Paper Technology, IIT Roorkee, Saharanpur Campus, which has been used for this work.

3.3.3 Electrospinning process optimization strategy

The step is to get an optimized condition of electrospinning parameters to get high quality bead free and low diametric nanofibers. It needs careful study of fiber formation.

In the first step, the effect of solution parameter such as polymer gelatin concentration (table 3.1) on nanofiber formation was studied to choose the best concentration to fabricate the fiber with best morphology. In the subsequent steps of the

optimization process effect of other spinning parameters (process and ambient) were studied to get the nanofiber of best morphology. The parameters such as flow rate, applied voltage, tip to collector distance (TCD), temperature and humidity were taken as the variation parameters to optimize the process. In several experimental conditions salt such as tetra ethyl ammonium chloride (1% w/v) was also added to the spinning solution prior to electrospinning to minimize the bead defect on nanofiber formation. Salt addition causes the additional charge injection to polymer solution causing enhancement of jet stability during the fiber formation.

3.4 Chemical integrity of drug in drug loaded electrospun nanofiber

Due to application of a high electrical potential to the drug containing gelatin solution during electrospinning, it is questionable whether the chemical integrity of drug would be intact after such a treatment. In order to verify that Fourier Transformation Infra Red (FTIR) spectroscopy method was employed to confirm the presence of drug in the electrospun nanofiber through functional group identification. The spectral peaks obtained from pure gelatin, pure drug and drug loaded gelatin nanofiber were compared to confirm the presence of drug molecule in the electrospun nanofiber mat.

3.5 In-vitro drug release study

3.5.1 Preparation phosphate buffer solution

9.6gms powdered form of PBS(without calcium and magnesium) was suspended in 900ml tissue culture grade water with constant, gentle stirring until the powder is completely dissolved without heating. pH was adjusted to 7.4 by using 1N HCL or 1N NaOH .The final volume is made to 1000ml by adding tissue culture grade water.

3.5.2 Preparation of standard calibration curve

1ml of drug solution (conc. 5mg/ml) is diluted to 10 times to make a solution of concentration of 1mg/ml which served as the stock for the preparation of calibration curve.

The calibration curve was carried out in the concentration range of 0.1-0.5mg/ml table 3.2 by adding required amount of stock to PBS buffer. Pure sample of PBS buffer serves as the control in the standard curve preparation.

Table 3.2 shows the composition of drug and phosphate buffer in solutions of different concentrations.

Table 3.2 *Composition of drug, PBS in the different concentration solution*

SL. No.	Concentration of drug in solution (%)	Total volume of solution(ml)	Amount of drug solution(ml)	Amount of drug (mg)	Amount PBS (ml)
1	0(control)	5	0	0	5
2	10	5	0.5	0.5	4.5
3	20	5	1	1	4
4	30	5	1.5	1.5	3.5
5	40	5	2	2	3
6	50	5	2.5	2.5	2.5

3.5.3 Drug release assay

Total immersion method was used to study the release characteristics of the amphotericin B from the drug loaded gelatin nanofiber mat. The drug loaded gelatin nanofiber mat containing a known quantity of amphotericin B (2.5mg) were fabricated under the optimized conditions of electrospinning. The mat was immersed in 150ml of phosphate buffer and incubated in a shaking water bath at the physiological temperature of 37°C. At a specified immersion period ranging from 0-12h period 0.5ml of buffer solution was taken out after each 0.5hr. The amount of drug in the withdrawn solutions was determined using UV Visible spectrophotometer at the wave length of 412nm as previously mentioned against the predetermined calibration curve. The calibration curve was carried out in the concentration range of 0.1-0.5mg/ml. The percentage of drug released during the study was calculated by comparing the release profile with the standard calibration curve.

Chapter 4

Results and Discussion

Formation of the drug loaded nanofibers were studied through electrospinning using different concentration of gelatin in acetic acid and water (4:1) mixed with 1 wt. % amphotericin B (based on the weight of the polymer). Several number of process optimization steps were followed by varying the different electrospinning parameters (process, solution and ambient parameters) to find the fibers with best morphology.

The fibers obtained under different electrospinning condition were analyzed with Field Emission Electron Microscopy (FE-SEM). The chemical integrity of drug, in fabricated drug loaded fibers were confirmed by FTIR spectroscopy and further drug release assay was studied in phosphate buffer of pH 7.4 at normal physiological temperature of 37°C.

4.1 Electrospinning process optimization and morphology of drug loaded fiber mat

The drug loaded fibers after prepared by the electrospinning process were dried in the desiccator filled with silica gel before FE-SEM observation. The effect of different electrospinning parameters on fiber morphology under different experimental conditions are depicted as below.

4.1.1. Effect of polymer concentration on fiber morphology

To study the impact of polymer concentration on fiber formation, polymer concentration is varied the range of 8-10%, but the other electrospinning conditions/parameters were kept unchanged as depicted below.

Conditions/parameters

Polymer: <i>Gelatin</i>	Tip to collector distance: <i>10cm</i>
Model drug: <i>Amphotericin B (1%)</i>	Humidity: <i>67%</i>
Volume flow rate: <i>0.1ml/h</i>	Temperature: <i>26°</i>
Applied voltage: <i>13KV</i>	Collector type: <i>Thick aluminum foil</i>

Figure 4.1, 4.2 and 4.3 shows the FE-SEM image results of electrospinning from the drug loaded gelatin solution using gelatin concentration of 8%, 9% and 10% respectively, following the above mentioned electrospinning conditions/parameters. The SEM micrographs of the fibers obtained by variation of polymer concentration shows the fiber formation tendency is very poor at lower concentration ranges such as 8% and 9% .

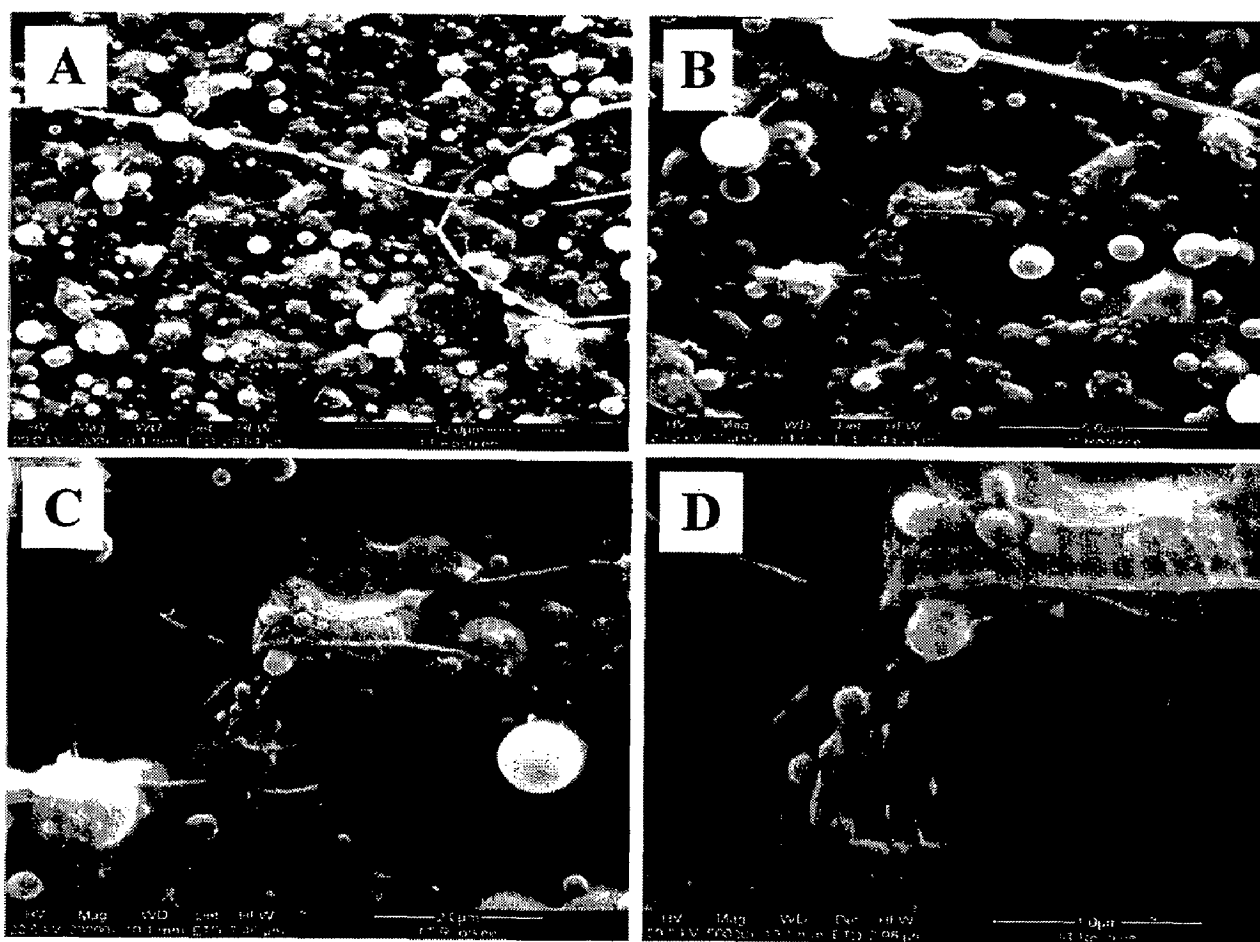


Fig:4.1 SEM images of amphotericin B loaded gelatin electrospun fibers from 8 wt% of gelatin in scale bar of 10 μm(A) , 5 μm(B), 2 μm(C) and 1 μm(D).

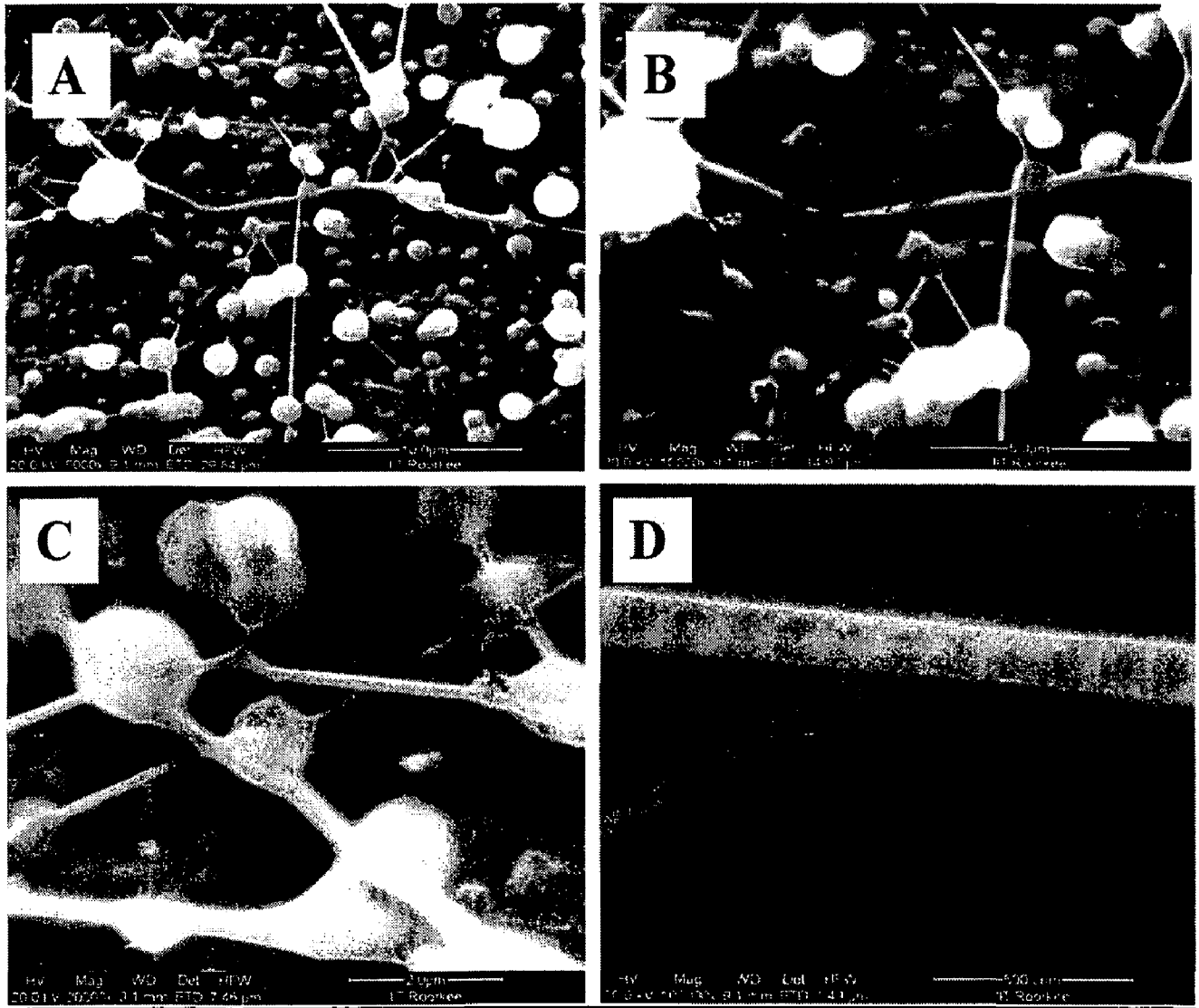


Fig:4.2 SEM images of amphotericin B loaded gelatin electrospun fibers from 9 wt% of gelatin in scale bar of 10 μm(A), 5 μm(B), 2 μm(C) and 0.5 μm(D)

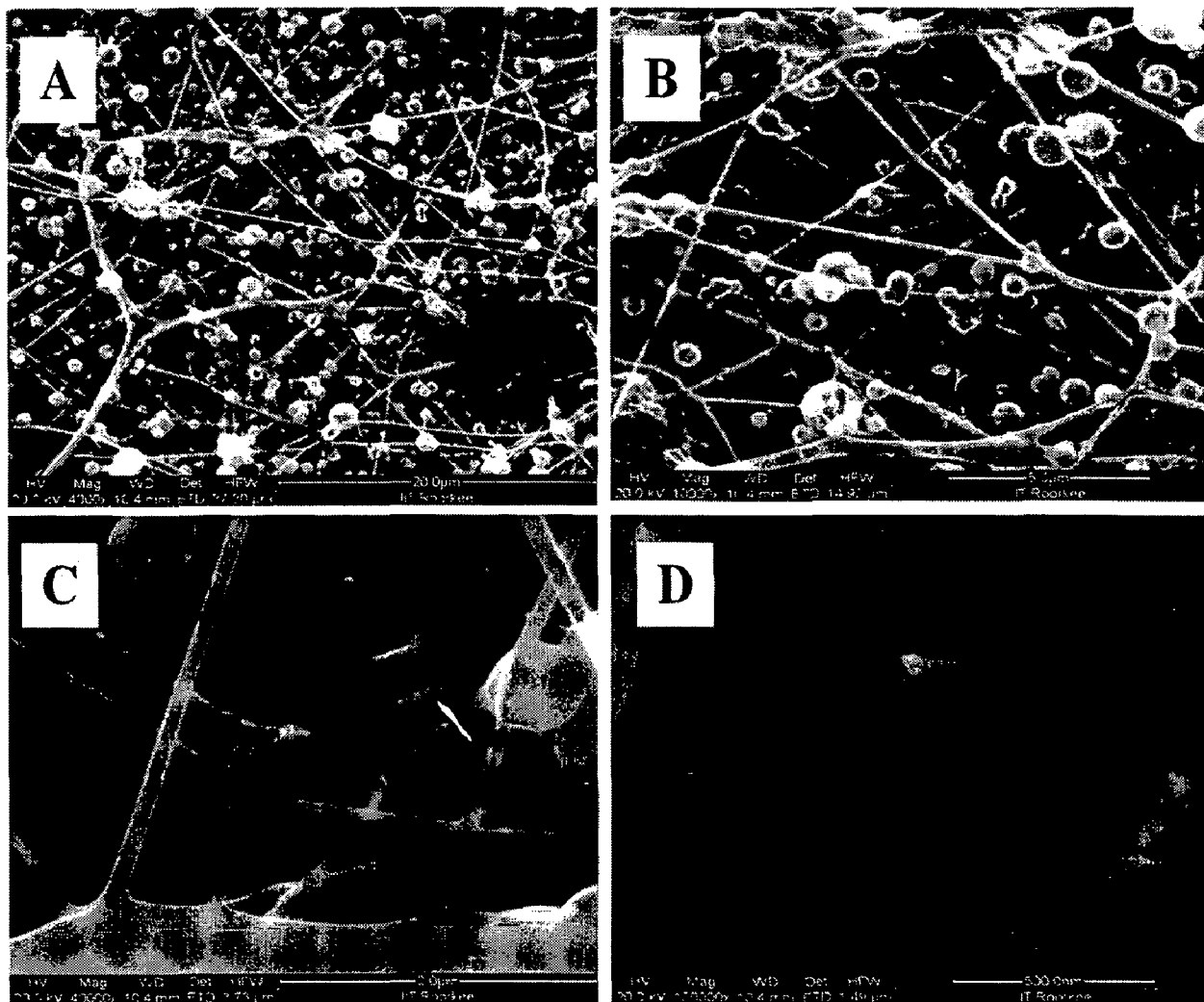


Fig:4.3 SEM images of amphotericin B loaded gelatin electrospun fibers from 10 wt% of gelatin in scale bar of 10 μm (A), 5 μm (B), 2 μm (C) and 0.5 μm (D)

It has been observed that the tendency of fiber formation increases towards the higher concentration of polymer and the concentration of 10% shows very good fiber formation with significant amount of beads. The poor fiber formation is due to the fact that, at lower concentration ranges the viscosity of the polymer is very low and as the concentration increases the viscosity of the spinning solution also increases, thereby affecting surface tension and viscoelastic behaviour of the solution. The viscosity affects the viscoelastic property of the fluid which is a very important factor for jet stability and chain entanglement to occur. Thus the polymer must have an effective concentration for chain

entanglement to occur. So, in this study 10% is the optimal range concentration of gelatin for effective chain entanglement. In subsequent step of experiments the polymer concentration of 10% was fixed and the other electrospinning parameters were varied to obtain bead free low diametric nanofibers. Salt of tetra ethy ammonium chloride(1%) was also added to control the beads.

4.1.2. Effect of volume flow rate on fiber morphology

To study the effect of volume flow rate/feed rate on fiber formation, the volume flow rate was varied the range of 0.1-0.4ml/hour where the other electrospinning conditions/parameters were kept unchanged as depicted below.

Conditions/parameters

Polymer: <i>Gelatin</i>	Tip to collector distance: <i>10cm</i>
Model drug: <i>Amphotericin B (1%)</i>	Humidity: <i>40%</i>
Polymer conc. (wt %): <i>10%</i>	Temperature: <i>26°</i>
Applied voltage: <i>13KV</i>	Collector type: <i>Iron metal grid</i>

Figure 4.4, 4.5, 4.6 and 4.7 shows the FE-SEM results of electrospinning from the drug loaded gelatin solution using 10 % gelatin with flow rate of 0.4, 0.3, 0.2 and 0.1 ml/hr respectively, following the above mentioned conditions. The SEM micrographs of the fibers obtained by variation of the volume flow rate suggests that the fiber diameter and bead defects increases with increasing flow rate from 0.1 to 0.4ml/hr and at very higher flow rate such as 0.4ml/hr the ribbon like fiber formation were notable rather than the fibers with circular cross section. This is because of incomplete fiber drying. The low diametric fiber and less bead formation at low flow rate is due to increase of viscoelastic property of the fluid because of increase in time period for solvent evaporation. The bead defects and fiber nonuniformity were still noticeable even at low flow rates because of inability of fibers to dry completely before reaching to collector. So the low bead volume is

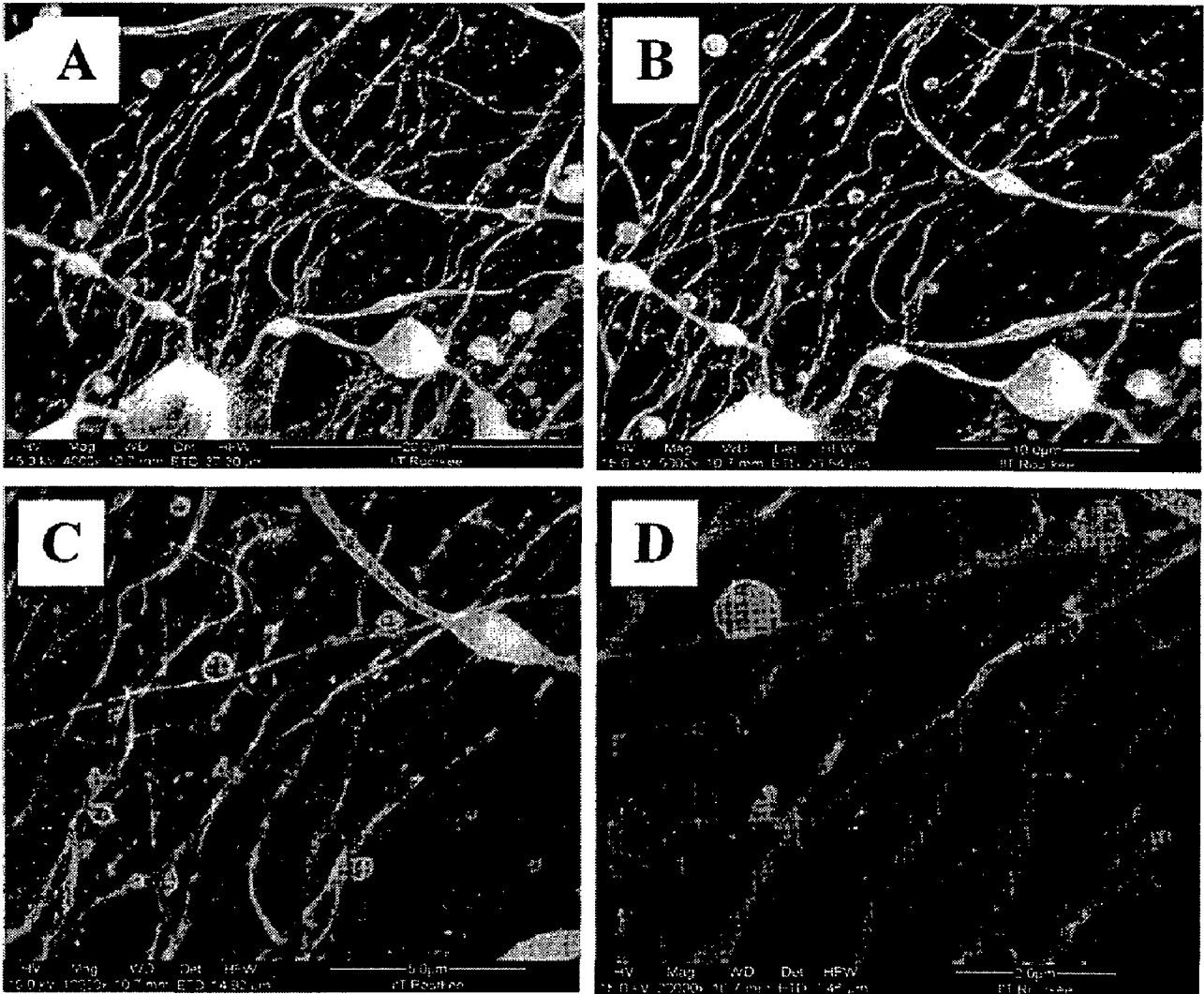


Fig:4.4 SEM images of amphotericin B loaded gelatin electrospun fibers from 10 wt% of gelatin at flow rate 0.4 ml/hr in scale bar of 20 μm(A), 10 μm(B), 5 μm(C) and 2μm(D)

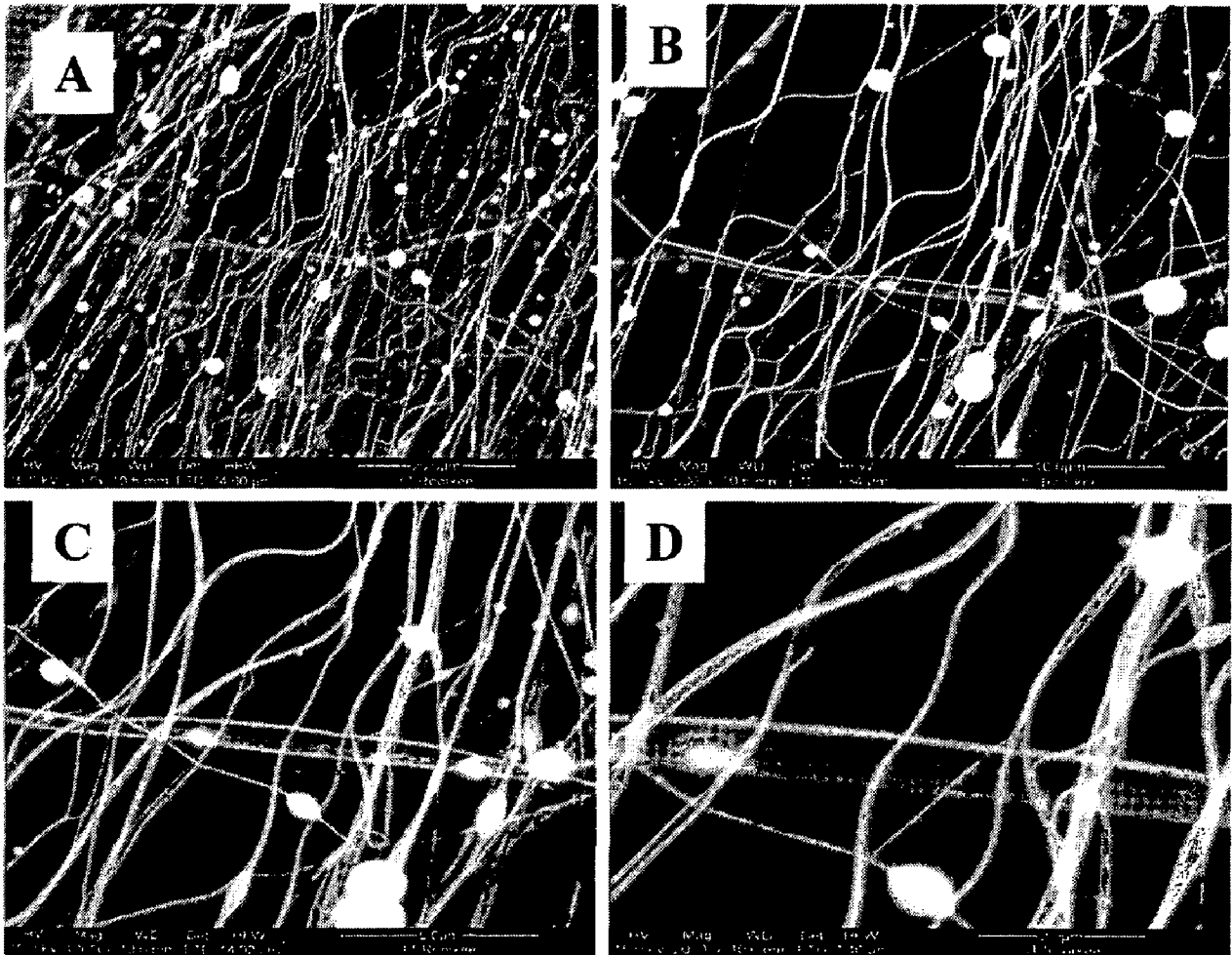


Fig:4.5 SEM images of amphotericin B loaded gelatin electrospun fibers from 10 wt% of gelatin at flow rate 0.3ml/hr in scale bar of 20 μm (A), 10 μm (B), 5 μm (C) and 2 μm (D)

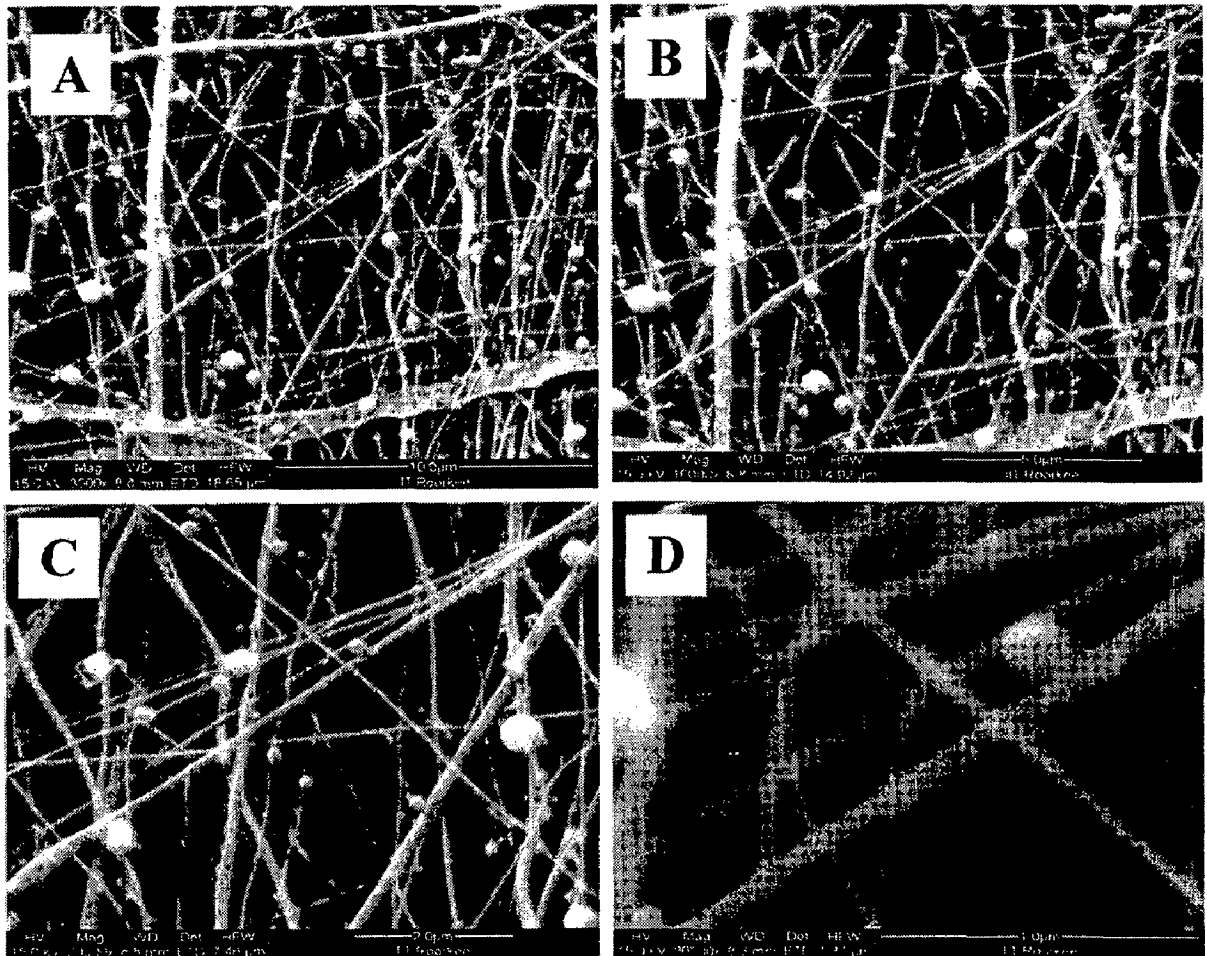


Fig:4.6 SEM images of amphotericin B loaded gelatin electrospun fibers from 10 wt% of gelatin at flow rate 0.2ml/hr in scale bar of 10 μm (A), 5 μm (B), 2 μm (C) and 1 μm (D)

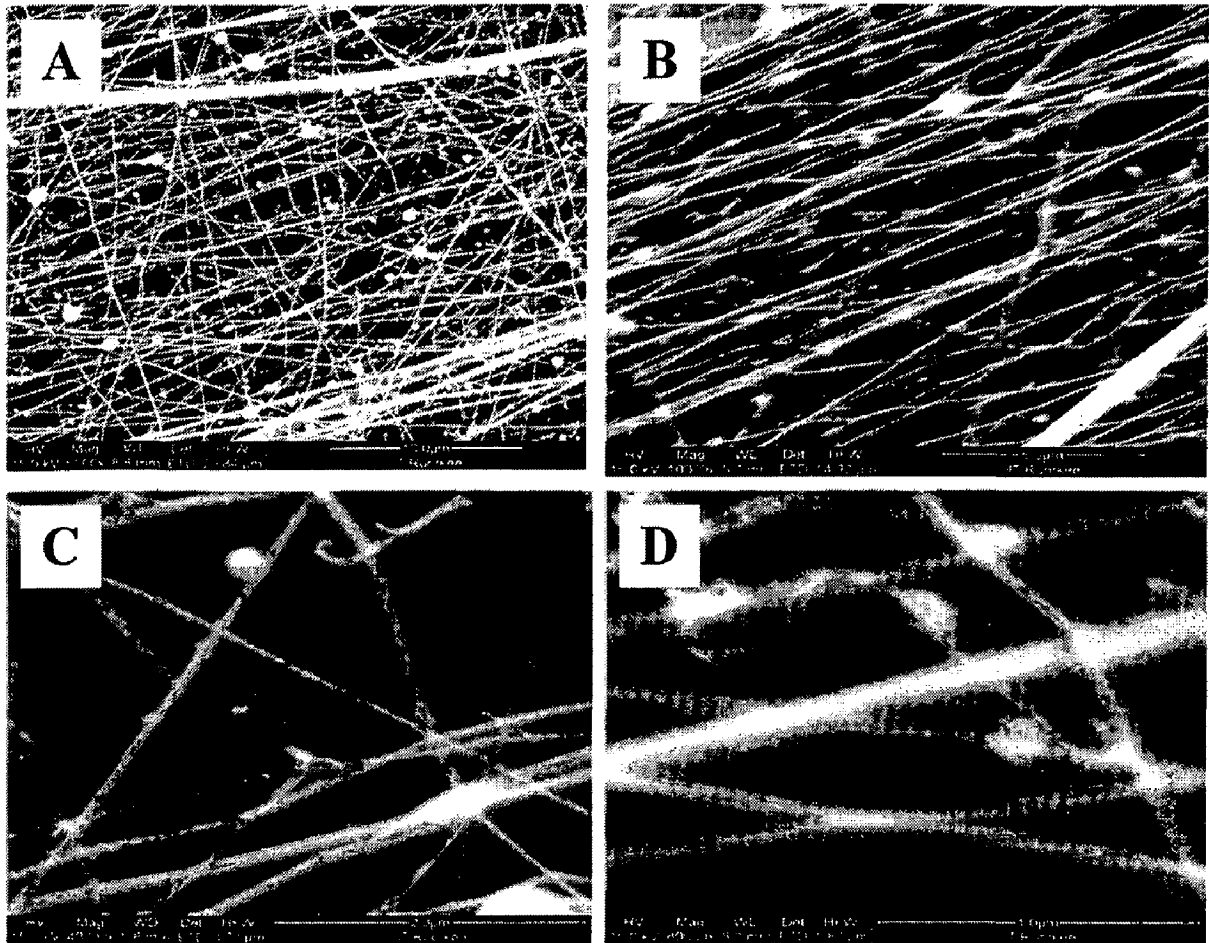


Fig:4.7 SEM images of amphotericin B loaded gelatin electrospun fibers from 10 wt% of gelatin at flow rate 0.1ml/hr in scale bar of 10 μm (A), 5 μm (B), 2 μm (C) and 1 μm (D)

attributed for not only the low flow rate but also addition of tetra ethyl ammonium salt(1%) and other ambient parameters such as humidity and temperature. The addition of salt enhances the charge on the polymer droplet. The extra charge build up is helpful for increasing the electrical force on the polymer droplet which is very much useful for overcoming the surface tension of the drop to form the Taylor cone. This increases the jet stability. Similarly temperature and humidity was also low in these experimental condition which has also some significant contribution over the bead control. At high humidity the fiber drying is critical which yields the fiber with beaded morphology. Thus the polymer flow rate has a high impact on fiber size. In this study the flow rate of 0.1 ml/hr yields the fibers of best morphology among all the flow rates. So in the subsequent steps of

experiment the flow rate of 0.1ml/hr was fixed where as the the tip to collector distance and applies voltage were varied to get the fibers of best morphology

4.1.3. Effect of applied voltage and tip to collector distance on fiber morphology

To study the effect of applied voltage and capillary/tip to collector distance on fiber morphology the formation of the fiber was tried in different applied voltage/tip to collector distance such as 20kV/12cm, 16kV/12cm, and 16kv/13.5cm where the other electrospinning conditions/parameters were kept unchanged as depicted below

Conditions/Parameters

Polymer: <i>Gelatin</i>	Humidity: 43%
Model drug: <i>Amphotericin B (1%)</i>	Temperature: 29°
Polymer conc. (wt %):10%	Collector type: <i>Iron metal grid</i>
Volume flow rate: 0.1 ml/hr	

Figure 4.8,4.9 and 4.10 shows the FE-SEM images for the electrospun fibers obtained from 10 wt% of gelatin at applied voltage/tip to collector distance of 20kV/12cm, 16kV/12cm, and 16kV/13.5cm respectively, following the above mentioned electrospinning conditions/parameters. It has been noticed that in all the cases the fibers were obtained with best morphology with very minimum quantity of bead. In some cases the bead defects were not observable. The strength of applied voltage were varied in the from 16kV to 20Kv(Fig:4.8,4.9 and 4.10). It has been observed that the high applied voltage is important for getting the fibers with low diameter and minimum quantity of beads where as a very high voltage like 20kV or higher, significant bead defects were noticeable(Fig:4.8). As the applied voltage increases the volume of the drop decreased until the Tayler cone was formed at the tip of the capillary, which was associated with an increase in bead defects seen among the electrospun nanofibers. The applied voltage of 16 kV is an optimal voltage to synthesize the fibers of very low diameter range and with very minimum quantity of the beads even in some cases no beads were observed.

Similarly the tip/Capillary to collector distance was varied in the range of 12-13.5cm(Figure 4.8,4.9 and 4.10). It has been noticed that, while playing a smaller role ,the

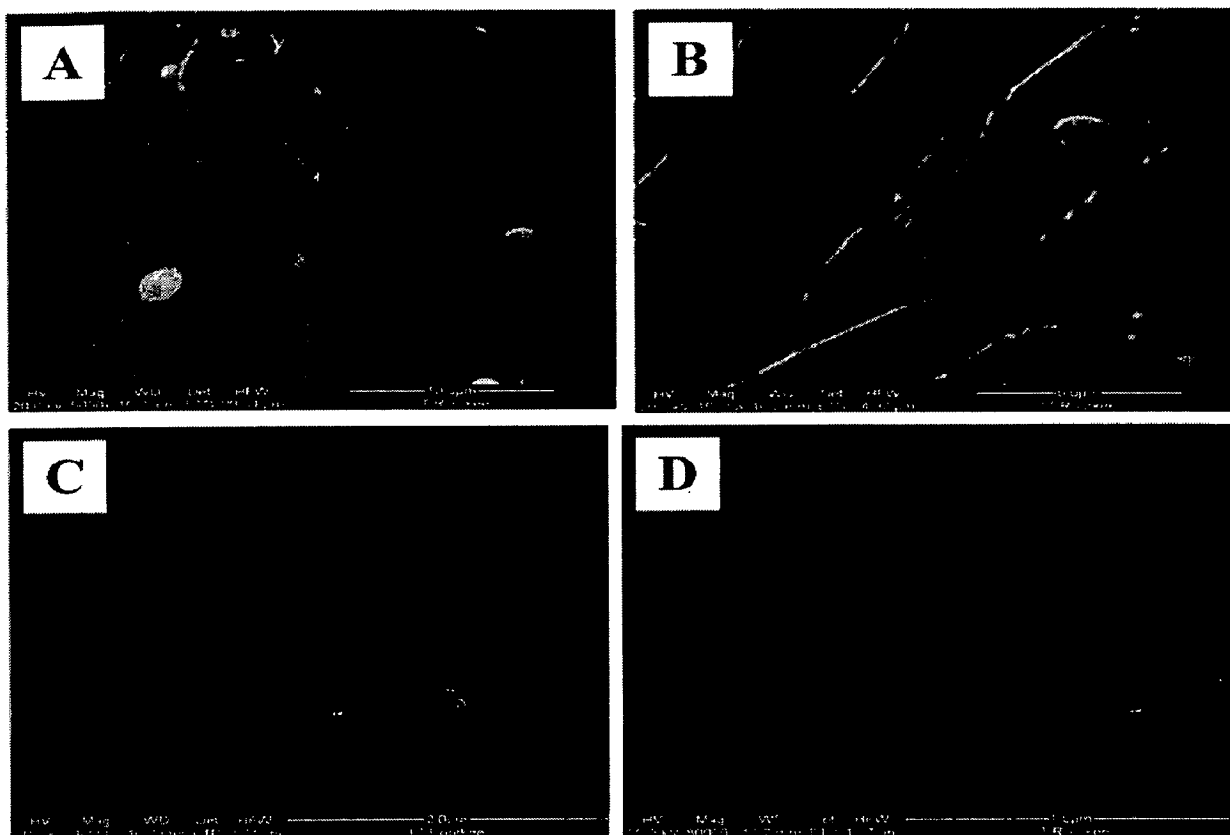


Fig:4.8 SEM images of amphotericin B loaded gelatin electrospun fibers from 10 wt% of gelatin at flow rate: 0.1ml/hr, applied voltage: 20kV, TCD: 12cm in scale bar of (A)10 μm , (B) 5 μm, (C) 2 μm and , (D)1 μm

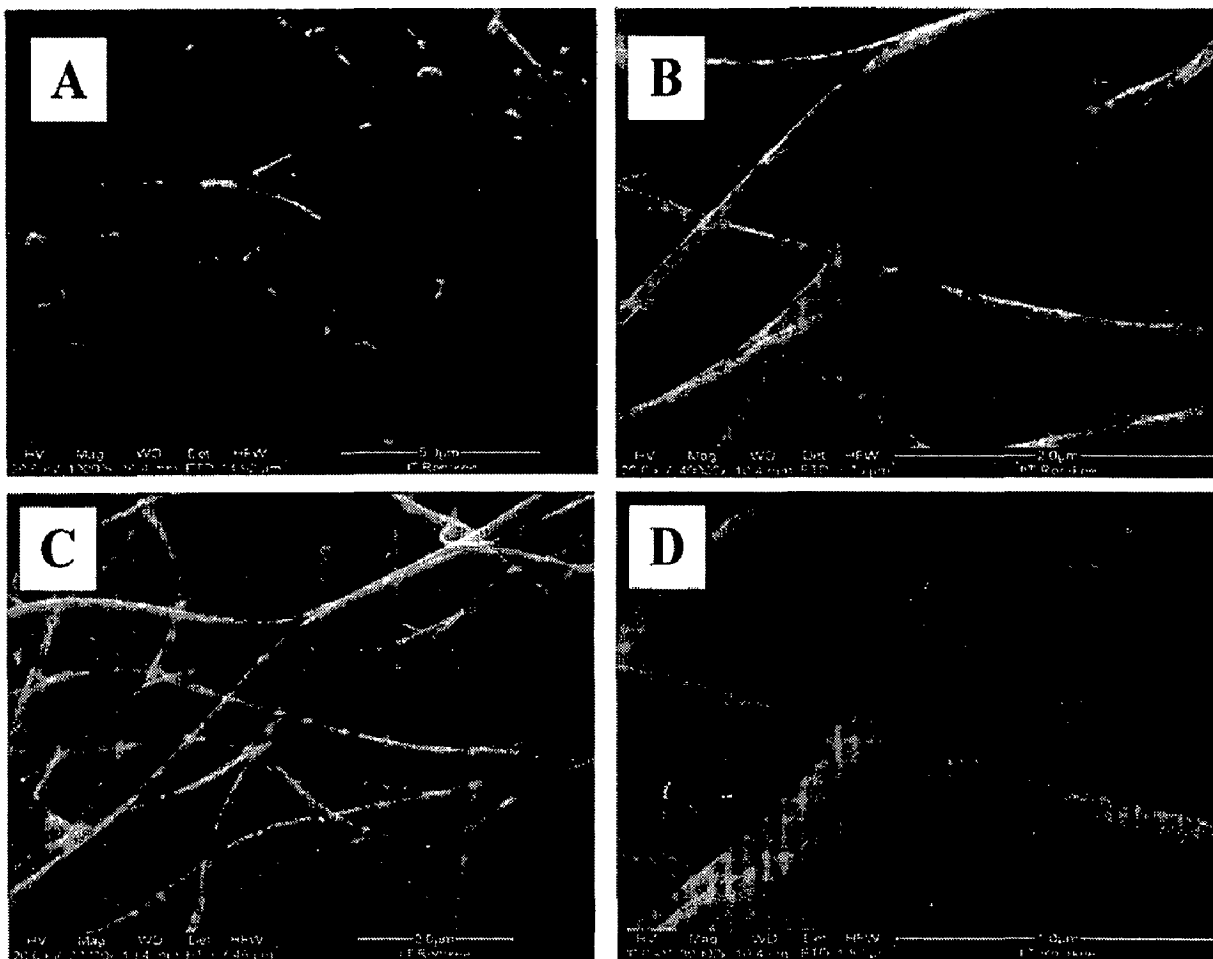


Fig:4.9 SEM images of amphotericin B loaded gelatin electrospun fibers from 10 wt% of gelatin at flow rate: 0.1 ml/hr, applied voltage: 20kV, TCD: 13.5cm in scale bar of 5 μm(A) , 2 μm(B), 2 μm(C) and , 1 μm(D)

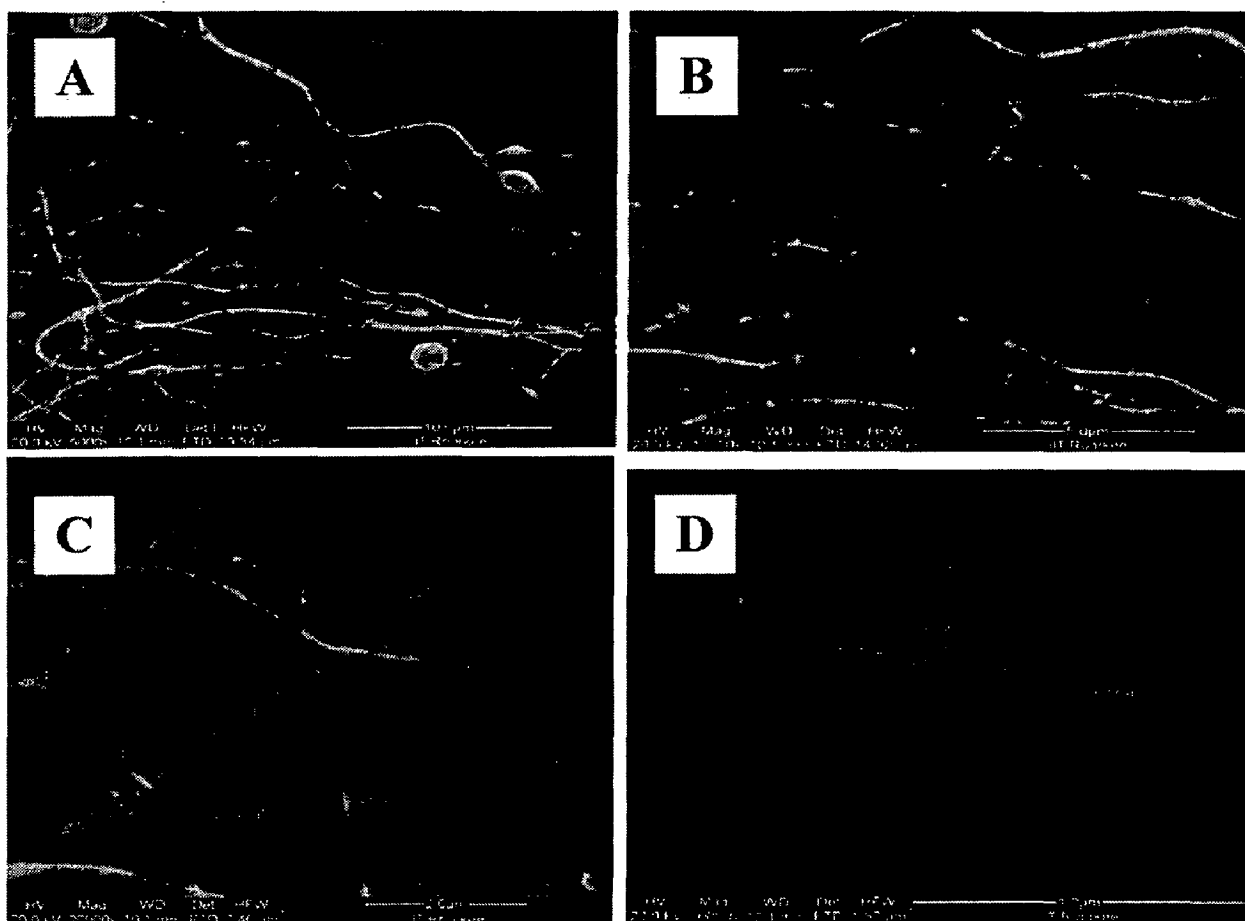


Fig:4.10 SEM images of amphotericin B loaded gelatin electrospun fibers from 10 wt% of gelatin at flow rate: 0.1ml/hr, applied voltage:16kV, TCD: 13.5cm in scale bar of 10 μm (A), 5 μm (B), 2 μm (C) and ,1 μm (D)

distance between capillary tip and collector can also influence the fiber diameter and also bead formation. The increase in capillary to collector distance from 12cm to 13.5cm at same applied voltage of 20kV(Fig.4.8 and 4.9) decreases the bead amount significantly. At this optimal range of the distance(13.5cm) the fiber formation occurs with extreme minimal amount of beads and with low diameter(average 100nm). Whereas short distance(Fig.4.8) is attributed to inadequate fiber drying before reaching at the collector. Figure 4.9 and 4.10 shows the fibers obtained at longer distance range of

13.5cm which shows very minimum bead defects due to adequate fiber drying than the fibers obtained at a distance of 12cm(Fig.4.8) or lower.

So in this optimization process, the drug loaded gelatin nanofibers of average diameter 100nm were fabricated by the advanced electrospinning process. The fibers thus obtained in this process were tested for the confirmation of chemical integrity of the drug in the spinned fiber by FTIR spectroscopic method.

4.2 Chemical integrity of drug in drug loaded gelatin nanofiber mat

The chemical integrity of drug in the drug loaded electrospun nanofiber was confirmed by Fourier Transformation Infra Red Spectroscopy (FTIR) technique. The figure 4.11, 4.12 and 4.13 shows the FTIR spectra obtained from pure amphotericin B,

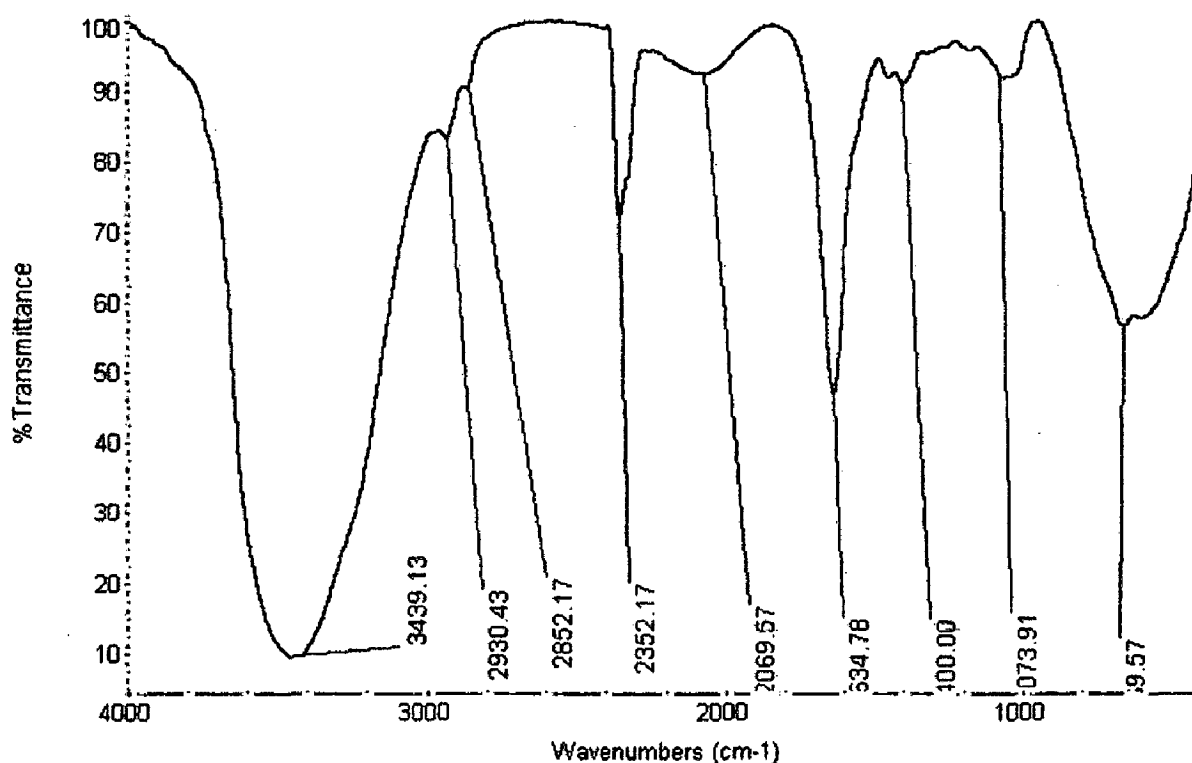


Fig:4.11 FTIR spectra of pure amphotericin B

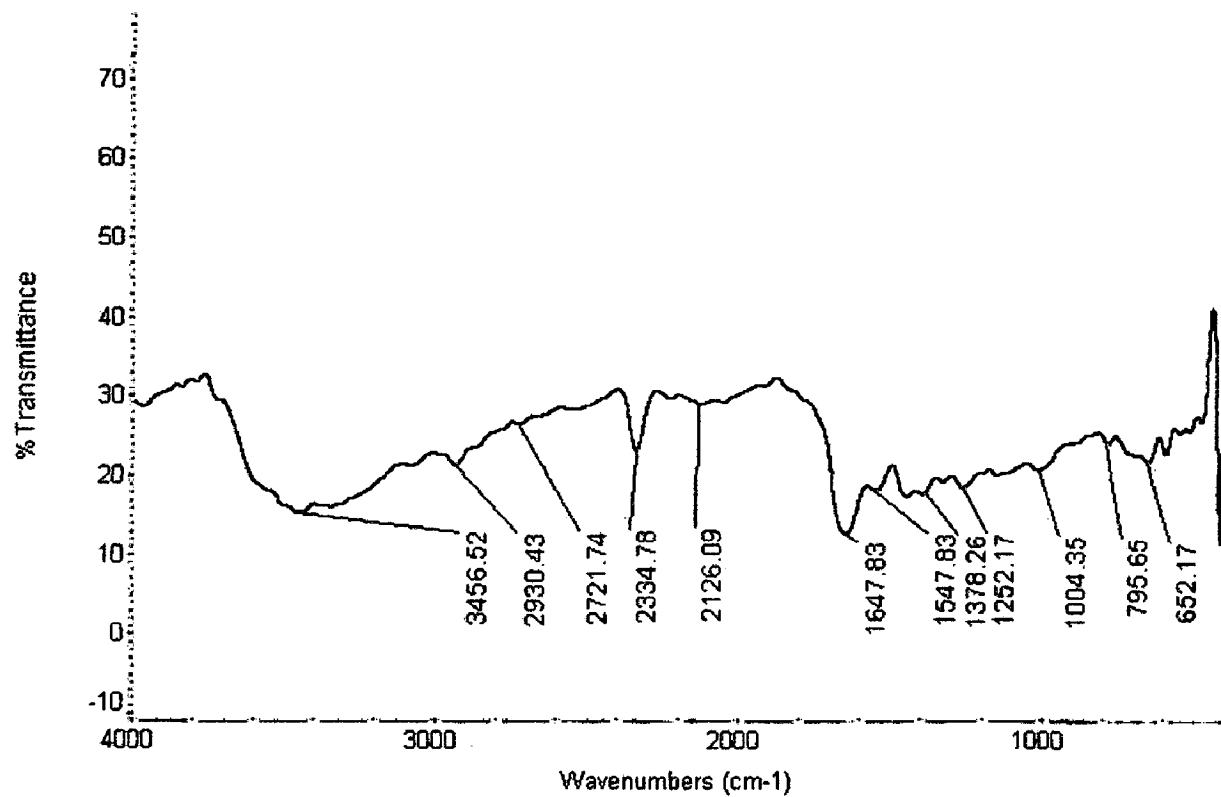


Fig:4.12 FTIR spectra of pure gelatin nanofiber

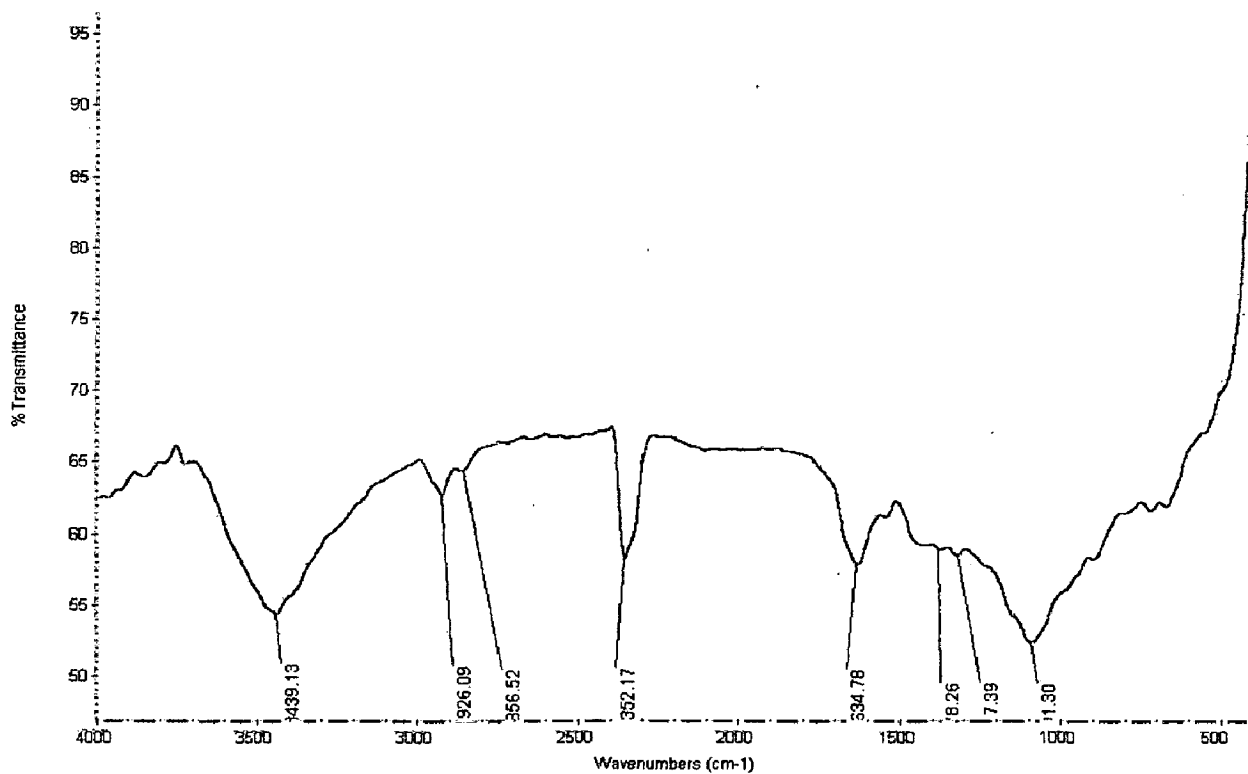


FIG:4.13 FTIR Spectra of amphotericin B loaded gelatin nanofiber

pure gelatin mat and amphotericin B loaded gelatin nanofiber mat. The FTIR spectral peaks of drug loaded nanofibers were compared with the spectral peaks obtained from pure amphotericin B and pure gelatin. The comparison shows that the presence of additional peak in the spectral region of drug loaded gelatin that correspond to CH₃ symmetric bending for R-CH₃ at FT-IR region of 1378.26 cm⁻¹. The spectral peak is present in gelatin but absent in the FT-IR spectra of pure drug. Similarly the presence of the peak corresponds to C=C stretching at FT-IR region of 1634.78 due to conjugated C=C in amphotericin B is observed in spectra of drug loaded gelatin fiber mat but absent in spectra of pure gelatin. Thus confirms the chemical integrity of the drug in electro-spun nanofiber.

4.3 In-vitro drug release study

4.3.1 Standard calibration curve preparation

The gelatin nanofibers mat containing a known amount of amphotericin B was fabricated under the obtained optimized conditions of electrospinning parameter. Prior to perform the drug release study a standard calibration curve is prepared with known quantity of drug samples in the concentration range of 0.1-0.5 mg/ml which correspond to the percentage concentration of drug in range of 10-50% in table 4.1. Pure phosphate buffer serves as the control in the standard curve preparation. The curve was prepared for knowing the exact quantity of drug that is released to the releasing medium during the release study.

Table 4.1 shows the optical absorbance of different concentration of drugs at 412nm (absorption maxima of amphotericin B) and figure 4.14 shows the standard calibration curve for the known drug concentrations

Table: 4.1 UV-Vis spectra analysis at different concentration of drug.

S. No.	Drug Concentration (%)	Absorbance at 412nm
1	0	0.000
2	10	0.300
3	20	0.566
4	30	0.789
5	40	0.964
6	50	1.179

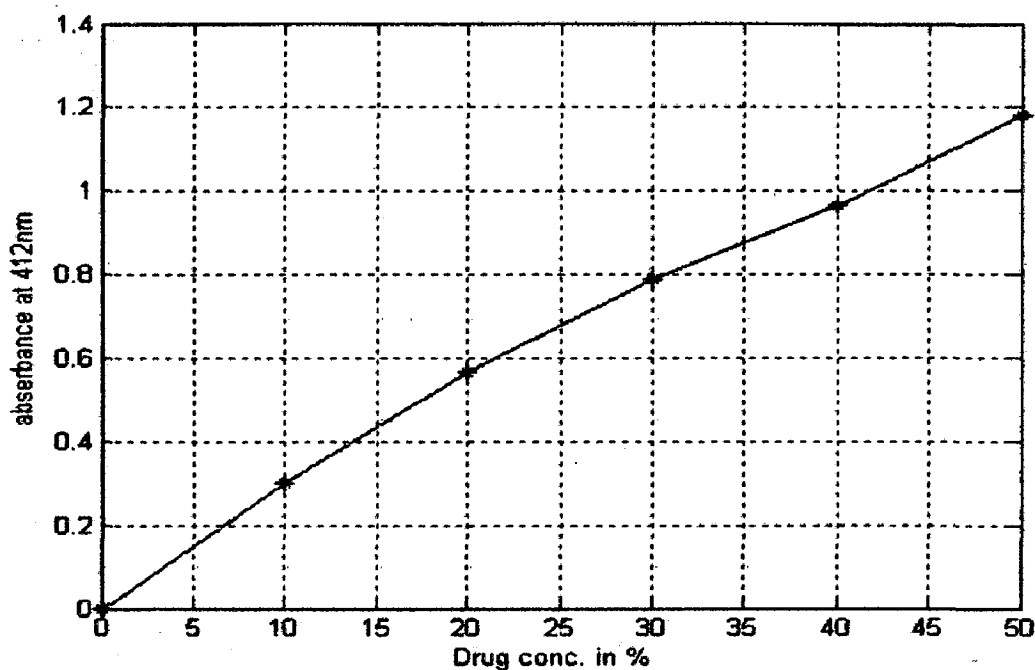


Fig:4.14 Standard calibration curve for the known drug concentrations

4.3.2 Drug release assay

The amphotericin B release was studied at 37° C in phosphate buffer at PH 7.4. The amphotericin B release profile from the electrospun gelatin nanofiber mat is shown in figure 4.15. The amount of drug release at each interval of 30 minutes was monitored with the help of a UV-Vis spectrophotometer and the corresponding absorbance at 412 nm is listed in table 4.2. The drug release profile in figure 4.15 represents, the release rate of amphotericin B at initial period up to three hours was very slow which is probably due to the diffusion of phosphate buffer into the nanofibers matrix, results in very slow leakage of drug molecules to come out of the solution. From fourth hour onwards it follows an exponential release up to 9.5th and from 9.5th hour onwards again the release is very slow and follows a nearly saturation stage at about 12th hour. The exponential release might be due to the fact that most of the solvent molecules from the outer environment have diffused into the nanofibers matrix to cause the highest leakage of the drug molecules to outside environment. Similarly, saturation phase is achieved due to equilibrium in diffusion process. Mathematically the diffusion term can be expressed in terms of *Fics Law of Diffusion*. The initial content of drug dissolved in spinning solution was 1 % (by weight of the polymer). After the drug assay it was found the drug of *approximately 60%*.

Table: 4.2 Observation of drug release in different time by UV-Vis spectroscopy

S. No.	Time (hrs)	Absorbance at 412nm
1	0	0.000
2	0.5	0.032
3	1	0.043
4	1.5	0.058
5	2	0.073
6	2.5	0.089
7	3	0.107
8	3.5	0.129
9	4	0.152
10	4.5	0.183
11	5	0.219
12	5.5	0.252
13	6	0.301
14	6.5	0.369
15	7	0.438
16	7.5	0.509
17	8	0.581
18	8.5	0.642
19	9	0.688
20	9.5	0.715
21	10	0.737
22	10.5	0.745
23	11	0.758
24	11.5	0.767
25	12	0.771

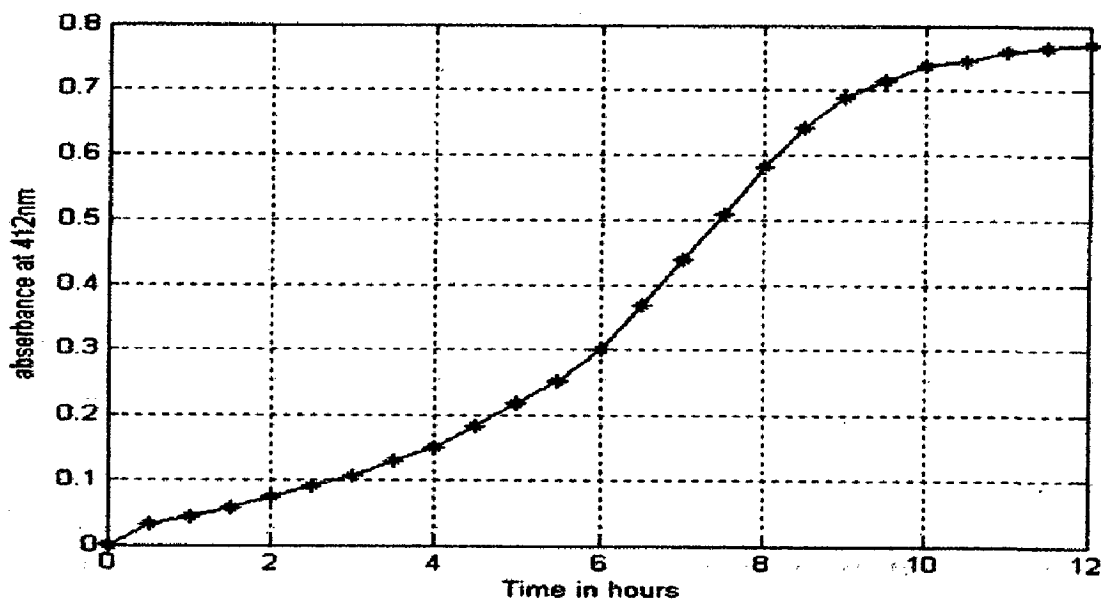


Fig:4.15 Drug release profile of amphotericin B in 12 hours

of the initial loading is released to the surrounding medium after twelve hours suggesting that the drug loading efficacy of such natural biodegradable nanofibers is very high. It may be concluded from the study that ‘the electrospun amphotericin B loaded gelatin based natural biodegradable nanofibers’ can act as a good delivery system for the model drug amphotericin B and might be promising for the treatment of leishmaniasis and severe fungal infections as alternative drug delivery devices.

Chapter 5

Summary

1. Electrospun nanofiber based new drug delivery system for amphotericin B as an antileishmanial and antifungal therapeutic was developed.
2. This system was based on encapsulation in electrospun nanofibers.
3. The fibers were natural and biodegradable polymers based on gelatin.
4. The successful to encapsulation and control release of the antifungal antibiotic amphotericin B through these natural and biodegradable polymeric nanofibers could be used for addressing the question about the nanodrug delivery system against leishmaniasis and several severe fungal infections.
5. The work also affords the opportunity to current era of tissue engineering research for fabrication of antifungal scaffold for cell attachment.

Chapter 6

Conclusion and Recommendation

Conclusion

The “**electrospun amphotericin B loaded gelatin based natural biodegradable nanofibers**” were successfully fabricated and the drug release study was performed over a period of twelve hours. The drug shows a slow release from the electrospun nanofiber which suggests, such natural and biodegradable nanofibers can be used as a **potential delivery system** for the medical drug **amphotericin B**. This might be promising for the treatment of leishmaniasis and severe fungal infections as alternative drug delivery devices.

Recommendation

1. In-vitro evaluation of the delivery system can be further evaluated by taking macrophages cell lines infected with *Leishmania sp.* and this nanocarrier system would be used against these cell lines. The drug would also be checked against the control cell lines without *Leishmania sp.* infection so as to evaluate its targeting potential.
2. After invitro evaluation, the system would be exposed to mouse models with *Leishmania sp.* for evaluation of infection, targeting, controlled release and curing potential. In addition, in-vivo imaging technique can be employed for knowing the targeting and controlled release potential of drug in mouse models.
3. Once drug attributes are optimized in mouse models clinical trials can be carried out.
4. In a similar way the other drugs that are available for leishmaniasis can also be tested through such delivery system for evaluation of therapeutic efficacy.
5. As in the present work, different types of biodegradable polymers can be developed to encapsulate these drugs for evaluating the therapeutic efficacy.

REFERENCES

- [1] Bhattacharyya A, Mukherjee M, Duttagupta S (2002) Studies on stibionate unresponsive isolates of *Leishmania donovani*, *J Biosci* 27:503-508.
- [2] Davies CR, Kaye P, Simon LC, Sundar S (2003) Leshmaniasis: new approaches to disease control, *BMJ* 326:377–82.
- [3] Rosenthal E, Marty P, Giudice P, Pradier C, Eastaut JA, Fichoux Y, Cassato JP (2000) RetroHIV and *Leishmania* co-infection: a review of 91 cases with focus on atypical location of *Leishmania*. *Clinical Infectious Diseases* 31: 1093–1095.
- [4] Faraut-Gambarelli F, Pioroux R, Deniau M, Giusiano B, Marty G, Faugere B, Dumon H (1997) In vitro resistance of *Leishmania infantum* to meglumine antimoniate: a study of 37 strains collected from patients with visceral leshmaniasis, *Antimicrob Agents Chemother* 41: 827–830
- [5] Lira R, Sunder S, Makharia A, Kenney R, Gam A, Saraiva E, Sack D (1999) Evidence that incidence of treatment failure in Indian kala-azar is due to the emergence of antimony resistant strains of *Leishmania donovani*, *J Infect Dis.* 180: 564–567.
- [6] Sundar S, Gupta LB, Makharia MK, Singh MK, Voss A, Rosenkaimer F, Engel J, Murray HW (1999) Oral treatment of visceral leshmaniasis with miltefosine, *Ann Trop Med Parasitol* 93: 589–597.
- [7] Mishra M, Biswas UK, Jha DN, Khan AB (1992) Amphotericin versus pentamidine in antimony-unresponsive kalaazar. *Lancet* 340: 1256–1257.
- [8] Perez-Victoria, F. J., Castanys, S. & Gamarro, F. (2003). *Leishmania donovani* resistance to miltefosine involves a defective inward translocation of the drug, *Antimicrob Agents Chemother* 47, 2397–2403.
- [9] Nwaka S. and Hudson A. Innovative lead discovery strategies for tropical diseases, *Nature Reviews Drug Discovery* 5, 941-955 (2006).
- [10] Croft SL, Sundar S, Fairlamb AH. Drug resistance in leshmaniasis, *Clinical microbiology reviews.* 2006 Jan; 19(1):111-26.
- [11] Eder L Romero & Maria Jose Morilla, *Expert Opin. Drug Deliv.* (2008) 5(7):805-823

- [12] Pattama Taepaiboon, Uracha Rungsardthong and Pitt Supaphol (2006) Drug-loaded electrospun mats of poly (vinyl alcohol) fibers and their release characteristics of four model drugs *Nanotechnology* 17 2317–2329
- [13] Santi Tungprapa, Ittipol Jangchud and Pitt Supaphol 2007 Release characteristics of four model drugs from drug-loaded electrospun cellulose acetate fiber mats, *Polymer* 48 5030-5041
- [14] Young S, Wong M, Tabata Y and Mikos A G 2005 Gelatin as a delivery vehicle for the controlled release of bioactive molecules *J. Control. Release* 109 256–74
- [15] Gisela Buschle-Diller, Jared Cooper, Zhiwei Xie, Ye Wu, James Waldrup, Xuehong Ren 2007 Release of antibiotics from electrospun bicomponent fibers *Cellulose*, 14:553–562
- [16] E.-R. Kenawy, G.L. Bowlin, K. Mansfield, J. Layman, D.G. Simpson, E.H. Sanders, G.E. Wnek, Release of tetracycline hydrochloride from electrospun poly(ethylene-co vinyl acetate), poly(lactic acid), and a blend, *Journal of Controlled Release* 81 (1–2) (2002) pp57–64.
- [17] X. Zong, K. Kim, D. Fang, S. Ran, B.S. Hsiao, B. Chu, Structure and process relationship of electrospun bioabsorbable nanofiber membranes, *Polymer* 43 (16) (2002) 4403–4412.
- [18] J. Zeng, X. Xu, X. Chen, Q. Liang, X. Bian, L. Yang, X. Jing, Biodegradable electrospun fibers for drug delivery, *Journal of Controlled Release* 92 (3) (2003) 227–231.
- [19] H. Jiang, D. Fang, B.S. Hsiao, B. Chu, W. Chen, Optimization and characterization of dextran membranes prepared by electrospinning, *Biomacromolecules* 5 (2) (2004) 326–333.
- [20] E.-R. Kenawy, F.I. Abdel-Hay, M.H. El-Newehy, G.E. Wnek, Controlled release of ketoprofen from electrospun poly (vinyl alcohol) nanofibers, *Materials Science and Engineering A* 459 (1–2) (2007) 390–396.
- [21] E Kenaway, F.I.Abdel-Hay, M.H.El-Newehy (2009) Processing of Polymer Nanofibers through Electrospinning as Drug Delivery Systems, I.Linkov and J.Steevens (eds), *Nanomaterials: Risks and Benefits @Springer Science+Business Media B.V.*

- [22] Giusti P, Barbani N, Lazzeri L, Polacco G, Crystallini C, Cascone MG. Gelatin-poly(Vinyl Alcohol) blends as bioartificial polymeric materials. Proceedings of the 4th international conference on Frontiers of Polymer and Advanced Materials, 4-9th January Cairo, Egypt; 1997
- [23] Banuls AL, Hide M, Franck Prugnolle *Leishmania* and the Leshmaniasis: A Parasite Genetic Update and Advances in Taxonomy, Epidemiology and Pathogenicity in Humans. *Advances in parasitology* 2007, 64: 1-109
- [24] Desjeux P: The increase in risk factors for leshmaniasis worldwide. *Transactions of the Royal Society of Tropical Medicine and Hygiene* 2001, 95: 239–243.
- [25] Desjeux P: Leshmaniasis: current situation and new perspectives. *World Health Stat Q* 1992, 45: 267-75.
- [26] Zijlstra EE, el-Hassan AM, Ismael A: Endemic Kala-azar in eastern Sudan: post-Kala-azar dermal leshmaniasis. *Am J Trop Med Hyg* 1995, 52:299-305
- [27] Lainson R, Shaw JJ: Evolution, classification and geographical distribution. In: *The Leishmaniasis in Biology and Medicine* 1987, Vol. 1: 1–120.
- [28] Lainson R, Shaw JJ, Silveira FT, de Souza AAA, Braga RR, Ishikawa EAY: The dermal leishmaniasis of Brazil, with special reference to the eco-epidemiology of the disease in Amazonia. *Memo'rias do Instituto Oswaldo Cruz* 1994, 89: 435–443.
- [29] Riera C, Fisa R, Udina M, Gallego M, Portus M: Detection of *Leishmania infantum* cryptic infection in asymptomatic blood donors living in an endemic area (Eivissa, Balearic Islands, Spain) by different diagnostic methods. *Transactions of the Royal Society of Tropical Medicine and Hygiene* 2004, 98: 102–110.
- [30] Reithinger R: Cutaneous leshmaniasis. *Lancet Infect Dis* Sep 2007, 7(9): 581-96.
- [31] Formhals A, inventor. Process and apparatus for preparing artificial threads. US Patent No. 1,975,504; 1934.
- [32] G. C. Rutledge, S. V. Fridrikh, *Adv. Drug Delivery Rev.* 2007, 59, 1384.
- [33] A. L. Yarin, S. Koombhongse, D. H. Reneker, *J. Appl. Phys.* 2001, 89, 3018.
- [34] D. H. Reneker, A. L. Yarin, H. Fong, S. Koobhongse, *J. Appl. Phys.* 2000, 87, 4531.
- [35] T. Han, D. H. Reneker, A. L. Yarin, *Polymer* 2007, 48, 6064.
- [36] M. M. Hohman, M. Shin, G. C. Rutledge, M. P. Brenner, *Phys. Fluid* 2001, 13, 2201.
- [37] M. M. Hohman, M. Shin, G. C. Rutledge, M. P. Brenner, *Phys. Fluid* 2001, 13, 2221.

- [38] S. V. Fridrikh, J. H. Yu, M. P. Brenner, G. C. Rutledge, *Phys. Rev.Lett.* 2003, 90, 144502.
- [39] Travis J. Sill, Horst A. von Recum 2008 *Electrospinning: Applications in drug delivery and Tissue Engineering Biomaterials* 29 1989-2006
- [40] Deitzel JM, Kleinmeyer J, Harris D, Tan NCB. The effect of processing variables on the morphology of electrospun nanofibers and textiles. *Polymer* 2001 Jan; 42(1):261e72.
- [41] Bognitzki M, Czado W, Frese T, Schaper A, Hellwig M, Steinhart M, et al. Nanostructured fibers via electrospinning. *Adv Mater* 2001; 13:70–2.
- [42] Andreas Greiner and Joachim H. Wendorff *Electrospinning: A Fascinating Method for the Preparation of Ultrathin Fibers Angew. Chem. Int. Ed.* 2007, 46, 2–36
- [43] E. R. Kenawy, G. L. Bowlin, K. Mansfield, J. Layman, D. G.Simpson, E. H. Sanders, G. E. Wnek, *J. Controlled Release* 2002, 81, 57.
- [44] Jingwei Xie, Chi-Hwa Wang, *Pharmaceutical Research*, Vol. 23, No. 8, August 2006
- [45]http://medpediamedia.com/u/Actigall-figure-01.jpg/Actigall-figure_01.jpg, dated June19, 2010
- [46]http://upload.wikimedia.org/wikipedia/commons/thumb/c/c8/Amphotericin_B_structure.svg/500px-Amphotericin_B_structure.svg.png dated June16, 2010.
- [47]http://www.stanford.edu/class/humbio103/ParaSites2003/Leishmania/Leishmania_LifeCycle.gif, dated 20th June 2010